**NIST Technical Note 2016**

# Spectrum Occupancy and Ambient Power Distributions for the 3.5 GHz Band Estimated from Observations at Point Loma and Fort Story

W. Max Lees
Adam Wunderlich
Peter Jeavons
Paul D. Hale
Michael R. Souryal

This publication is available free of charge from:
https://doi.org/10.6028/NIST.TN.2016

National Institute of Standards and Technology
U.S. Department of Commerce

**NIST Technical Note 2016**

# Spectrum Occupancy and Ambient Power Distributions for the 3.5 GHz Band Estimated from Observations at Point Loma and Fort Story

W. Max Lees
Adam Wunderlich
Peter Jeavons
Paul D. Hale
Michael R. Souryal
*Communications Technology Laboratory*

This publication is available free of charge from:
https://doi.org/10.6028/NIST.TN.2016

September 2018
INCLUDES UPDATES AS OF 11-19-2018; SEE APPENDIX A


U.S. Department of Commerce
*Wilbur L. Ross, Jr., Secretary*

National Institute of Standards and Technology
*Walter Copan, NIST Director and Undersecretary of Commerce for Standards and Technology*

**National Institute of Standards and Technology Technical Note 2016**
**Natl. Inst. Stand. Technol. Tech. Note 2016, 69 pages (September 2018)**
**CODEN: NTNOEF**

**This publication is available free of charge from:**
**https://doi.org/10.6028/NIST.TN.2016**

NASCTN Report 5

NIST Technical Note 2016

# Spectrum Occupancy and Ambient Power Distributions for the 3.5 GHz Band Estimated from Observations at Point Loma and Fort Story

W. Max Lees
Adam Wunderlich
Peter Jeavons
Paul D. Hale
Michael R. Souryal
*Communications Technology Laboratory, NIST*

September 2018
INCLUDES UPDATES AS OF 11-19-2018; SEE APPENDIX A

# NASCTN

National Advanced Spectrum and Communications Test Network

## National Advanced Spectrum and Communications Test Network (NASCTN)

The mission of the National Advanced Spectrum and Communications Test Network (NASCTN) is to provide, through its members, robust test processes and validated measurement data necessary to develop, evaluate and deploy spectrum sharing technologies that can increase access to the spectrum by both federal agencies and non-federal spectrum users.

NASCTN was formed to provide a single focal point for engaging industry, academia, and other government agencies on advanced spectrum technologies, including testing, measurement, validation, and conformity assessment. NIST hosts the NASCTN capability at the Department of Commerce Boulder Laboratories in Boulder, Colorado.
NASCTN is a membership organization under a charter agreement. Members

- Make available, in accordance with their organization's rules policies and regulations, engineering capabilities and test facilities, with typical consideration for cost.
- Coordinate their efforts to identify, develop and test spectrum sharing ideas, concepts and technology to support the goal of advancing more efficient and effective spectrum sharing.
- Make available information related to spectrum sharing, considering requirements for the protection of intellectual property, national security, and other organizational controls, and, to the maximum extent possible, allow the publication of NASCTN test results.
- Ensure all spectrum sharing efforts are identified to other interested members.

Current charter members are:

- National Institute of Standards and Technology (NIST)
- Department of Defense Chief Information Officer (DoD CIO)
- National Telecommunications and Information Administration (NTIA)
- National Oceanic and Atmospheric Administration (NOAA)
- National Science Foundation (NSF)

# Abstract

This report presents descriptive statistics characterizing a set of over 14,000 spectrograms that were recorded by a recent measurement campaign at two coastal locations: Point Loma, in San Diego, California and Fort Story, in Virginia Beach, Virginia. Specifically, occupancy and vacancy statistics are compiled for each 10 MHz channel in which a primary federal incumbent system in the 3.5 GHz band (3550-3700 MHz), the shipborne SPN-43 air traffic control radar, was observed. In addition, empirical ambient (SPN-43 absent) power density distributions are presented for each multiple of 10 MHz between 3440-3670 MHz. These descriptive statistics are potentially informative to federal regulators and commercial users of the Citizens Broadband Radio Service that permits commercial wireless networks to share spectrum with federal users in the 3550-3700 MHz band in the United States.

# Contents

# Acronyms

**CBRS** Citizens Broadband Radio Service
**CBS** cavity-backed spiral
**CCDF** complementary cumulative distribution function
**CDF** cumulative distribution function
**CNN** convolutional neural network
**ESC** environmental sensing capability
**FCC** Federal Communications Commission
**OOBE** out-of-band emissions
**ROC** receiver operating characteristic
**SAS** spectrum access system
**STFT** short-time Fourier transform

# List of Figures

# Chapter 1

# Introduction

Plans are proceeding in the United States for commercial wireless usage of the 3550-3700 MHz ("3.5 GHz") band. Specifically, the U. S. Federal Communications Commission (FCC) has adopted rules for the Citizens Broadband Radio Service (CBRS) [1] to facilitate spectrum sharing between commercial users and federal incumbents. Key components of the CBRS framework include a spectrum access system (SAS) and environmental sensing capability (ESC) detectors.

The purpose of the SAS is, among other things, to coordinate commercial-user CBRS access so that federal incumbents are given priority. The primary federal incumbents in the 3.5 GHz band are shipborne and ground-based radars operated by the U.S. Department of Defense [2]. The CBRS framework requires that ESC sensors detect these radars, including the SPN-43 air traffic control radar [3], also identified as Shipborne Radar 1 in [2]. ESC detection capabilities are determined by intended and unintended emissions, as well as background noise. For example, out-of-band emissions (OOBE) from an adjacent-band U.S. Navy radar, identified as Shipborne Radar 3 in [2], are prevalent [4–7], and could complicate SPN-43 detection.

Distributions for SPN-43 spectrum occupancy and ambient (SPN-43-absent) power estimated from field measurements are potentially informative to both federal regulators and commercial industry, as they may be relevant to ESC requirements [8, 9] and ESC development efforts. Namely, the distribution of time-intervals in which the channel is occupied or vacant may be relevant to a requirement that the channel be vacated for a fixed time-interval after incumbent signals have been detected [8]. Distributions of ambient power may be relevant to ESC developers since some detection strategies may result in unacceptably high false-alarm rates for channels with higher levels of non-SPN-43 emissions. In addition, field observations of ambient power levels are relevant to ESC certification testing [9], since they could inform selection of background noise levels.

This report provides channel occupancy and ambient power distributions derived from a set of

14,739 spectrogram recordings in the 3.5 GHz band obtained during a recent measurement campaign [6, 7] at two coastal locations: Point Loma, in San Diego, California and Fort Story, in Virginia Beach, Virginia. Specifically, we present empirical distributions for SPN-43 spectrum occupancy and vacancy time-intervals for every 10 MHz channel in which SPN-43 was detected. In addition, using SPN-43-absent measurements, we present empirical distributions for the ambient power spectral density at each multiple of 10 MHz between 3440 MHz and 3670 MHz.

The results given here build on work presented in [10], which developed and trained deep learning classifiers for SPN-43 detection. In particular, we apply the best-performing classifier, a convolutional neural network (CNN), to label the complete set of spectrograms with respect to SPN-43 presence. The comprehensive set of plots given in this report complement the limited set of results provided in [10].

# Chapter 2

# Methods

## 2.1 3.5 GHz Spectrograms

As detailed in two technical reports [6, 7], 3.5 GHz band measurements were collected for a period of two months at Point Loma, in San Diego, California and for two months at Fort Story, in Virginia Beach, Virginia. The results presented here are derived from a set of 14,739 spectrograms collected approximately every ten minutes as part of that measurement effort. In total, roughly 58% of the spectrograms were acquired in San Diego and 42% in Virginia Beach. At each measurement site, data were collected with both an omni-directional antenna and a directional, cavity-backed spiral (CBS) antenna. Approximately 45% and 55% of the spectrograms were acquired with the omni-directional and CBS antennas, respectively [10].

The spectrograms each span a time-interval of 60 seconds and 200 MHz in frequency. The frequency coverage for most spectrograms is roughly 3465-3665 MHz, but due to variations in the receiver local oscillator frequency setting and the pre-selector filter, the frequency range covered by the complete set of measurements is 3435-3670 MHz. Each spectrogram has dimensions $134 \times 1024$, with 134 time-bins of duration 0.455 seconds and 1024 frequency-bins approximately 220 kHz wide. The spectrogram values were computed by applying a short-time Fourier transform (STFT) [11, p. 866] to I/Q data samples and then retaining the maximum amplitude in each frequency bin (i.e., max-hold) over each 0.455 second time-epoch. Details on the STFT windowing as well as steps used to convert spectrogram values to power spectral density units (dBm/MHz) are given in [10].

The spectrogram frequencies used for our analysis were determined by the frequency responses of the pre-selector and receiver [6, 7]. Specifically, the intersection of the passband for the pre-selector with the passband for the receiver anti-aliasing filter was used to define the range of valid

measurement frequencies. The pre-selector used for all of the measurements in San Diego and for the Virgina Beach measurements with the CBS antenna had a passband of 3427-3671 MHz, where these frequencies correspond to the -3 dB points in the frequency response. The pre-selector filter used for the Virginia Beach measurements with the omni-directional antenna had a passband of 3480-3665 MHz. The receiver anti-aliasing filter conservatively had a 200 MHz wide passband, centered on the local oscillator frequency, which was set to different values throughout the measurement campaign.

The measurements were collected with various receiver reference level values. Therefore, because different receiver front-ends were used at each site, the receiver noise floor depended both on the selected reference level and the measurement site. Table 2.1 lists the max-hold spectrogram noise floor for each reference level and measurement site. The values in Table 2.1 were derived from Table 2.4 in [6] and Table 2.4 in [7], for San Diego and Virgina Beach, respectively. Namely, the values given in [6, 7] were converted from dBm/Hz to dBm/MHz by (i) adding 60 dB for the Hz-MHz conversion, and (ii) adding 10.9 dB to convert from average to peak power; see the footnote on p. 32 of [6, 7].

Figure 2.1 shows example spectrograms. In each spectrogram, leakage from the local oscillator of the receiver is faintly visible as a vertical line at 3577 MHz (Top and Middle) and 3565 MHz (Bottom). The top spectrogram shows a clean capture of a strong SPN-43 radar emission, located at approximately 3570 MHz. Periodic radar sweeps are visible roughly every 4 seconds, corresponding to the SPN-43 antenna rotation period. The middle and bottom spectrograms of Figure 2.1 give examples of coincident Radar 3 OOBE and SPN-43. In these images, Radar 3 OOBE are visible as horizontal streaks, and weak SPN-43 emissions are visible at 3570 MHz (Middle) and 3550 MHz (Bottom), respectively. See [6, 7] for additional examples.

| Reference Level (dB) | San Diego (dBm/MHz) | Virginia Beach (dBm/MHz) |
|---|---|---|
| 5 | -84.7 | -87.2 |
| 0 | N/A | -90.6 |
| -10 | -94.7 | -94.8 |
| -20 | -96.8 | -96.0 |
| -30 | -97.7 | -96.4 |

Table 2.1: The max-hold spectrogram noise floor corresponding to each reference level and measurement site. Note that no data was collected at the 0 dB reference level in San Diego.

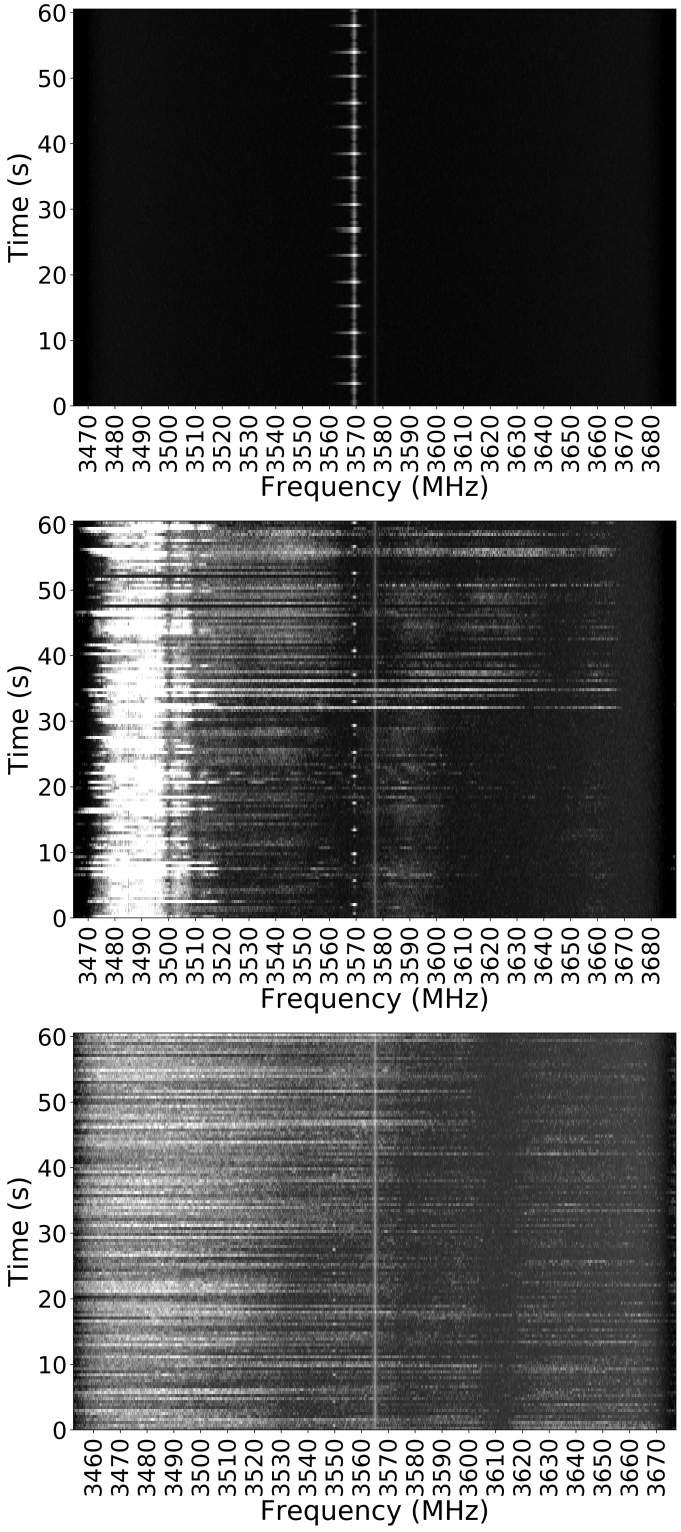


Figure 2.1: Example spectrogram captures. (Top) Strong SPN-43 emissions near 3570 MHz; grayscale window [-90 -50] dBm (Middle) Radar 3 OOBE coincident with SPN-43 emissions near 3570 MHz; grayscale window [-95 -75] dBm (Bottom) Radar 3 OOBE coincident with weak SPN-43 emissions near 3550 MHz; grayscale window [-95 -75] dBm.

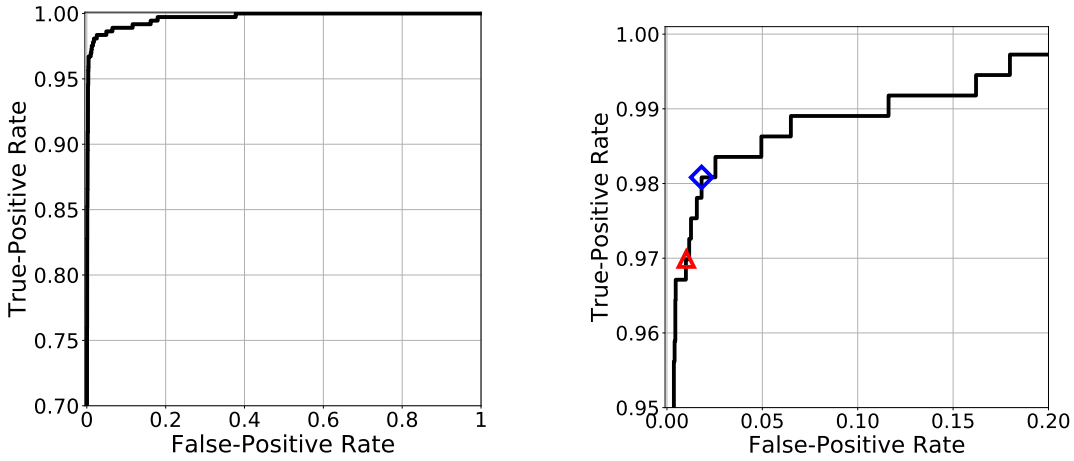


Figure 2.2: Empirical ROC curve for the CNN applied to single-channel SPN-43 detection. Left: Full ROC curve. Right: Zoom of ROC curve. The red triangle denotes the operating point used for SPN-43 occupancy estimation. The blue diamond denotes the operating point used for ambient (SPN-43 absent) power density estimation.

## 2.2 SPN-43 Radar Detection

In order to estimate SPN-43 occupancy statistics and power density distributions when SPN-43 was absent, we first had to identify all SPN-43 instances in our spectrogram library. From the complete set of 14,739 spectrograms, 4,491 were labeled by a human for SPN-43 presence. It should be emphasized that the human-applied labels were unverified, and based on subjective visual interpretation, as we did not have access to ship locations or assigned frequencies during or after the measurements. As described in [10], a subset of the human-labeled spectrograms was utilized to train a CNN detection algorithm, which was then applied to generate SPN-43 labels for every 10 MHz channel in the remaining unlabeled spectrograms.

For a single-channel detection task, where the aim is to detect SPN-43 in a given 10 MHz-wide channel, Figure 2.2 (left) shows the empirical receiver operating characteristic (ROC) curve for the CNN applied to "test set A" in [10]. The ROC curve plots the true-positive rate versus the false-positive rate over all detection thresholds [12,13]. To generate spectrogram labels, it was necessary to choose a detection threshold. To balance the trade-off between limiting false-positives and limiting false-negatives (missed-detections), we used different decision thresholds to generate SPN-43 labels prior to estimating channel occupancy and ambient power distributions, respectively. In the following sections, we give details on the applied detection thresholds and the rationale behind their selection.

## 2.3 Occupancy and Vacancy Interval Estimation

As stated above, spectrograms were collected roughly every ten minutes. This sampling interval was not exact due to hardware restrictions, like the rate at which data could be saved to disk, which increased the sampling interval by at most one minute. Despite this fact, to simplify our estimates of vacancy and occupancy time-intervals, we assumed that the captures were exactly ten minutes apart. To calculate the length of time a 10 MHz channel was either occupied by SPN-43 or vacant, we ordered the spectrograms by their capture time and then counted the number of consecutive vacant and occupied observations per channel. These counts were then multiplied by 10 minutes to generate the estimated durations. Note that this approach could not resolve changes in SPN-43 occupancy that occurred less than 10 minutes apart. Also, we did not attempt to quantify the potential bias due to nonuniformities in the sampling interval.

In addition to occupancy and vacancy time-intervals, we estimated the occupancy ratio, i.e., the total amount of time the channel was occupied by SPN-43 divided by the total capture time. Uncertainties shown for these estimates are approximate 95% confidence intervals obtained using the classical Wald interval for a binomial proportion [14].

To generate SPN-43 labels for the purpose of estimating channel occupancy and vacancy, we chose a CNN decision threshold that controlled the false-positive rate. Namely, we used the decision threshold corresponding to the false-positive rate closest to 1% on our test set. (Note that because different thresholds lead to discrete-valued false-positive and true-positive rates on a test set, there is no threshold corresponding exactly to the desired false-positive rate of 1%.) This operating point is marked with the red triangle on the zoom ROC plot in Figure 2.2 (right). The true-positive rate at this threshold is approximately 97%.

Because we controlled false-positives at the potential expense of additional false-negatives (missed SPN-43 detections), our estimates of occupancy and vacancy time-intervals are negatively and positively biased, respectively. Histograms of occupancy and vacancy intervals for each channel where SPN-43 was observed are provided in Chapter 3.

## 2.4 Ambient Power Distribution Estimation

To generate SPN-43 labels for the purpose of estimating ambient (SPN-43 absent) power distributions, we chose to control the rate of missed detections (false-negatives) at the potential expense of additional false-positives. Specifically, we used the decision threshold corresponding to the false-negative rate closest to 2% on our test set. Because the false-negative rate is equal to one minus the true-positive rate [13], this operating point corresponds to a true-positive rate near 98%; the false-

positive rate is approximately 1.8%. The operating point is marked with the blue diamond on the zoom ROC plot in Figure 2.2 (right). The decision to control missed SPN-43 detections was motivated by the fact that missed detections would likely add a positive bias to SPN-43 absent power distribution estimates. SPN-43 generally has higher power than the noise floor of our data. So, the result of including missed detections in our SPN-43 absent power distribution estimates would have been the inclusion of higher power captures, skewing our data towards higher values. Furthermore, because false-positives only slightly decreased the number of available SPN-43-absent observations, the cost of excluding them from the SPN-43 absent sample was small.

After classification of the unlabeled spectrograms, the channels found to contain SPN-43 were discarded. The remaining spectrogram values were converted to peak-detected spectral power density units (dBm/MHz) as described in Section 2.1, and used to estimate the empirical cumulative distribution function (CDF) for the power density in the 220 kHz-wide frequency-bin nearest to each multiple of 10 MHz. A nonparametric, simultaneous 95% confidence band was estimated for the empirical CDF using a method based on the Dvoretzky-Kiefer-Wolfowitz inequality; see [15, Thm. 7.5] for details. Also, we estimated empirical percentiles with associated $95\%$ confidence intervals derived from the simultaneous 95% confidence band. Semi-log plots of each complementary cumulative distribution function (CCDF), equal to one minus the CDF, as well as percentile tables are provided in Chapter 4.

# Chapter 3

# Results: Occupancy and Vacancy

We present occupancy and vacancy statistics for each 10 MHz channel that contained a SPN-43 observation. For San Diego, the observed signals were centered at 3520 MHz, 3550 MHz, and 3600 MHz. For Virginia Beach, they were centered at 3570 MHz, 3600 MHz, and 3630 MHz. Aggregated results for San Diego and Virginia Beach are given at the end of the chapter.

Each figure in this section contains histograms for time-intervals of continuous SPN-43 occupancy and vacancy in the 10 MHz channel centered at the specified frequency. The histograms focus on time-intervals lasting less than 120 minutes. This cut-off was selected because it corresponds to a proposed requirement that a channel be vacated by commercial wireless networks for 120 minutes after detection of an incumbent signal [8, p. 64, R2-ESC-12]. In addition, there is a table that lists the total number of occupancy and vacancy time-intervals that were used to generate the histograms, the occupancy ratio, i.e., the total amount of time the channel was occupied by SPN-43 divided by the total capture time, the number of continuous occupancy and vacancy time-intervals that exceeded 120 minutes, and the median, 75th and 99th percentiles of the occupancy and vacancy time-interval distributions. For the aggregated results at the end of the chapter, the occupancy ratio should be interpreted as the proportion of time any 10 MHz channel in which SPN-43 emissions were observed at a given location was occupied. Namely, for any channel where SPN-43 was observed in San Diego and Virginia Beach, there was an 11.4% and a 9.2% chance, respectively, that the channel was occupied.

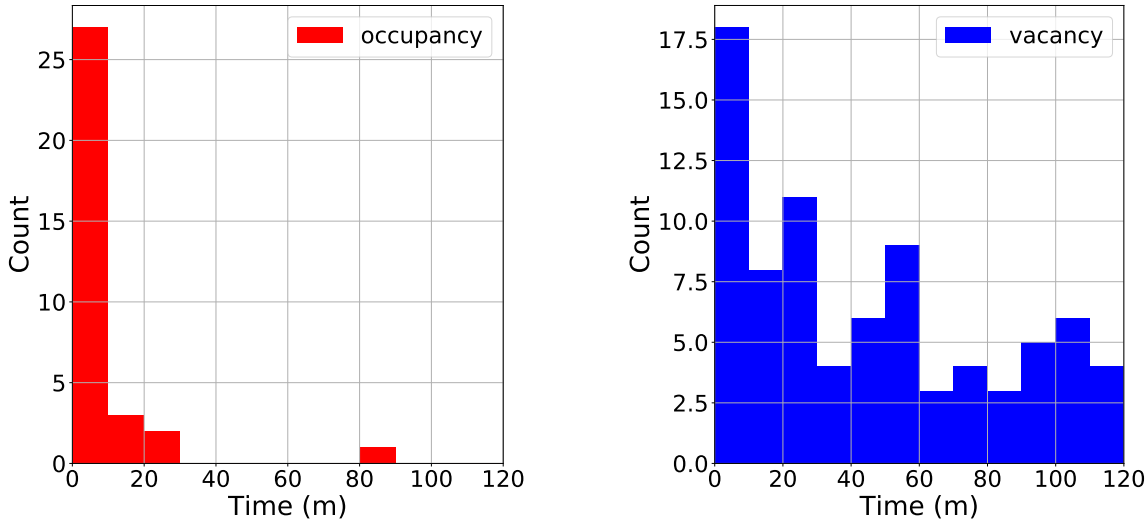


| Type | Total | Occupancy Ratio | $> 120$ min | Median (min) | 75th Pct (min) | 99th Pct (min) |
|---|---|---|---|---|---|---|
| Occupancy | 38 | $0.036 \pm 0.002$ | 5 | 10 | 20 | 778 |
| Vacancy | 204 | | 123 | 10 | 20 | 1990 |

Figure 3.1: (Left) Occupancy and (Right) Vacancy histogram of SPN-43 in the 3520 MHz channel in San Diego. (Bottom) Summary statistics.

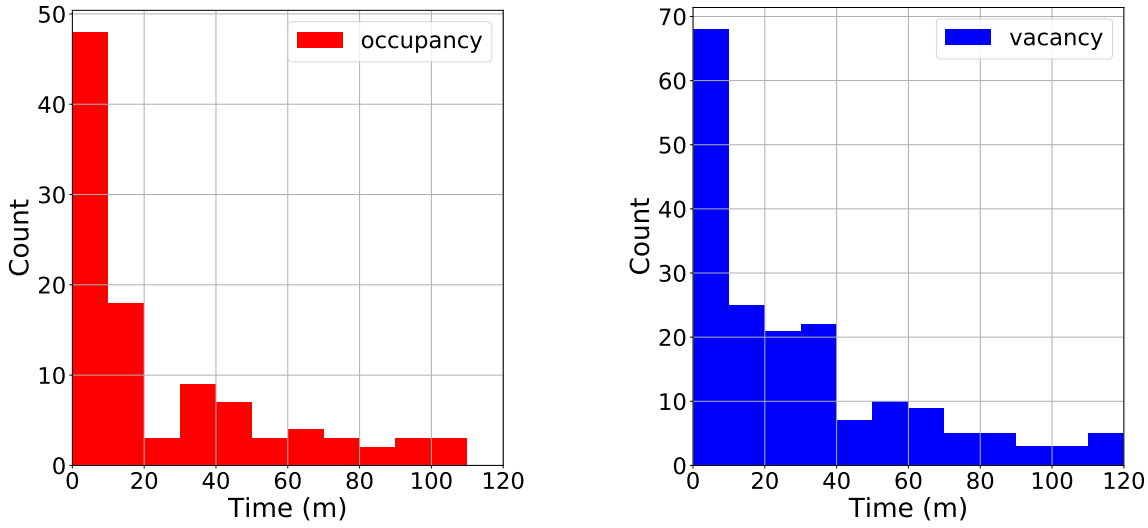


| Type | Total | Occupancy Ratio | $>$ 120 min | Median (min) | 75th Pct (min) | 99th Pct (min) |
|---|---|---|---|---|---|---|
| Occupancy | 127 | $0.287 \pm 0.005$ | 24 | 20 | 90 | 3630 |
| Vacancy | 321 | | 138 | 70 | 230 | 1450 |

Figure 3.2: (Left) Occupancy and (Right) Vacancy histogram of SPN-43 in the 3550 MHz channel in San Diego. (Bottom) Summary statistics.

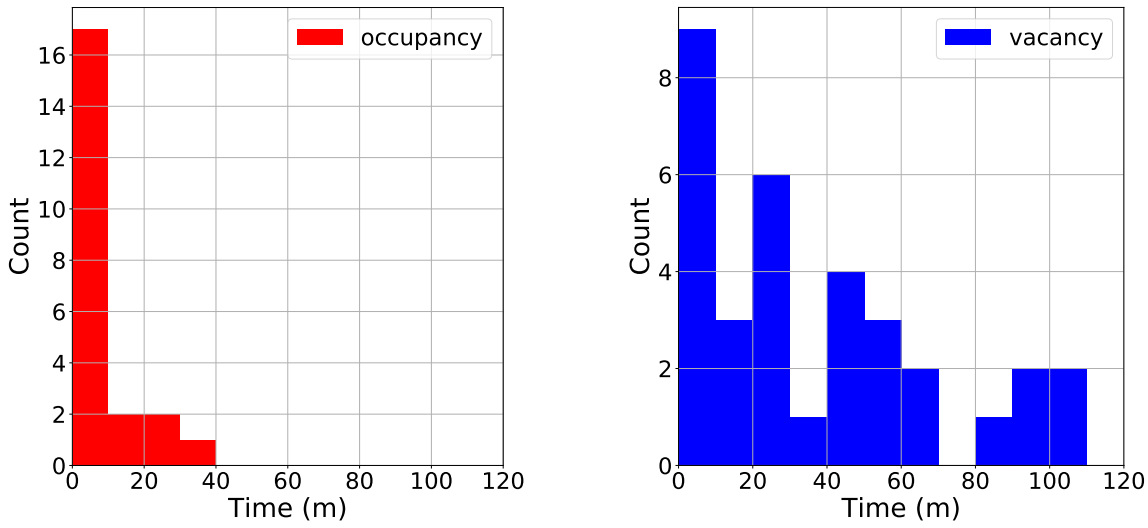


| Type | Total | Occupancy Ratio | $> 120$ min | Median (min) | 75th Pct (min) | 99th Pct (min) |
|---|---|---|---|---|---|---|
| Occupancy | 26 | $0.018 \pm 0.001$ | 4 | 10 | 30 | 440 |
| Vacancy | 98 | | 65 | 410 | 1100 | 5420 |

Figure 3.3: (Left) Occupancy and (Right) Vacancy histogram of SPN-43 in the 3600 MHz channel in San Diego. (Bottom) Summary statistics.

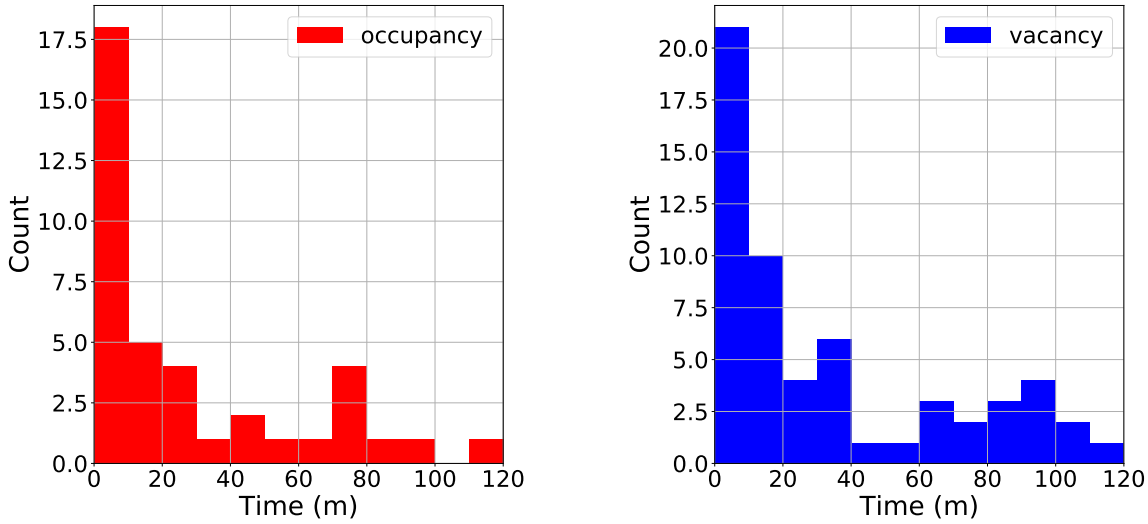


| Type | Total | Occupancy Ratio | $>$ 120 min | Median (min) | 75th Pct (min) | 99th Pct (min) |
|---|---|---|---|---|---|---|
| Occupancy | 52 | $0.116 \pm 0.004$ | 13 | 30 | 120 | 910 |
| Vacancy | 108 | | 50 | 100 | 610 | 3130 |

Figure 3.4: (Left) Occupancy and (Right) Vacancy histogram of SPN-43 in the 3570 MHz channel in Virginia Beach. (Bottom) Summary statistics.

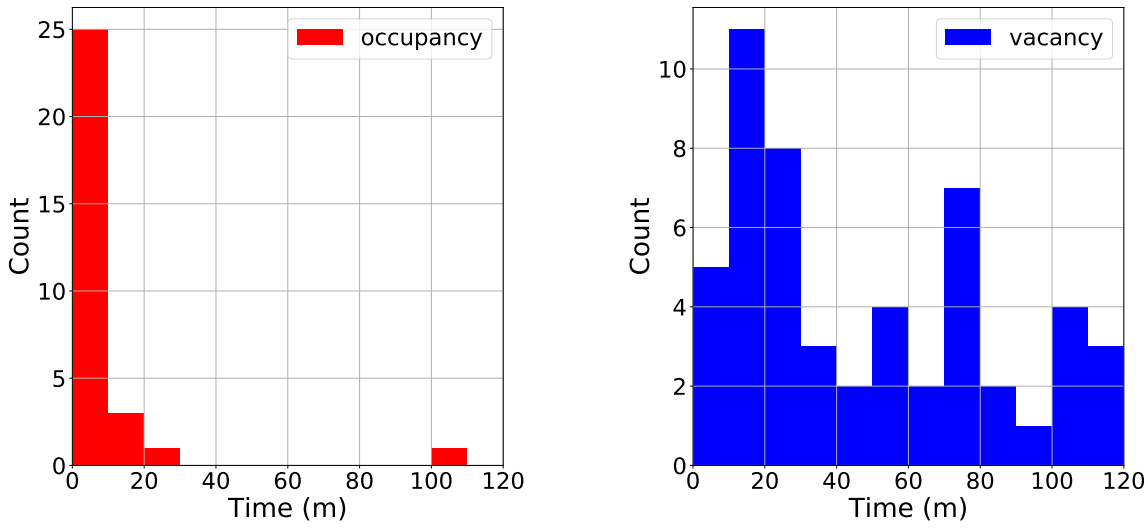


| Type | Total | Occupancy Ratio | $>$ 120 min | Median (min) | 75th Pct (min) | 99th Pct (min) |
|---|---|---|---|---|---|---|
| Occupancy | 37 | $0.118 \pm 0.004$ | 7 | 10 | 20 | 2010 |
| Vacancy | 121 | | 69 | 180 | 350 | 4150 |

Figure 3.5: (Left) Occupancy and (Right) Vacancy histogram of SPN-43 in the 3600 MHz channel in Virginia Beach. (Bottom) Summary statistics.

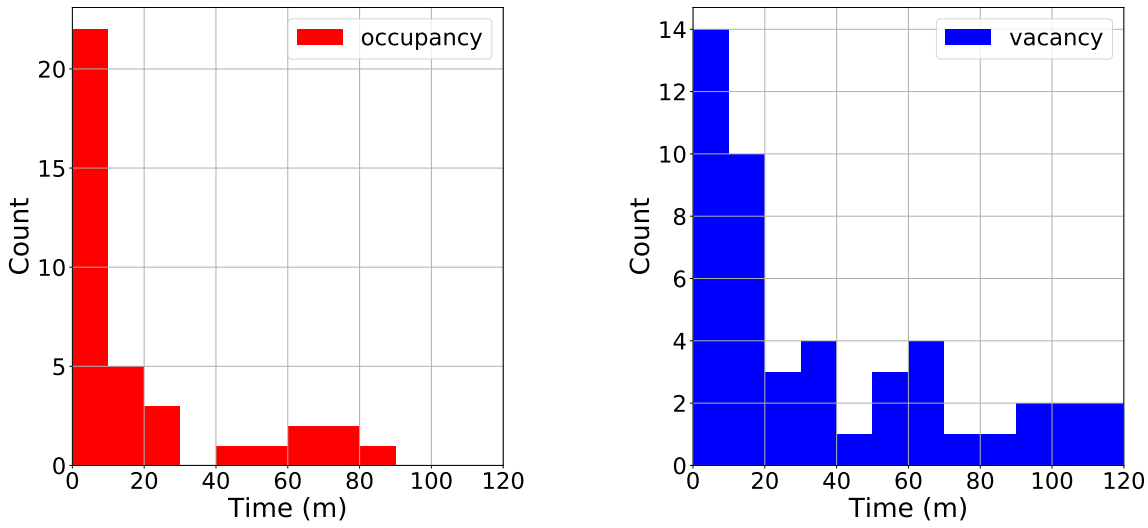


| Type | Total | Occupancy Ratio | $>$ 120 min | Median (min) | 75th Pct (min) | 99th Pct (min) |
|---|---|---|---|---|---|---|
| Occupancy | 44 | $0.041 \pm 0.003$ | 7 | 20 | 70 | 360 |
| Vacancy | 93 | | 46 | 120 | 430 | 5820 |

Figure 3.6: (Left) Occupancy and (Right) Vacancy histogram of SPN-43 in the 3630 MHz channel in Virginia Beach. (Bottom) Summary statistics.

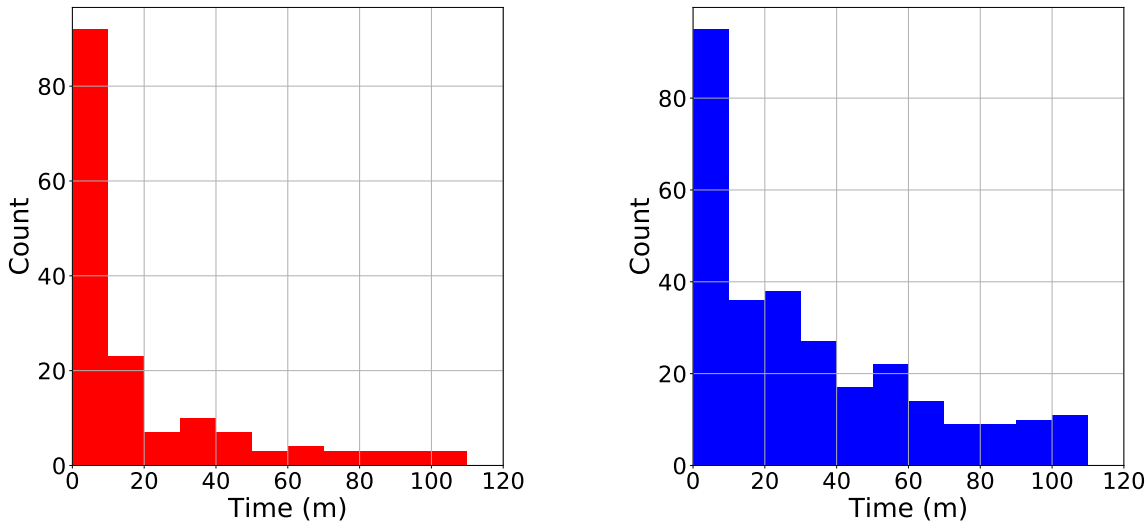


| Type | Total | Occupancy Ratio | $>$ 120 min | Median (min) | 75th Pct (min) | 99th Pct (min) |
|---|---|---|---|---|---|---|
| Occupancy | 191 | $0.114 \pm 0.002$ | 33 | 20 | 70 | 2460 |
| Vacancy | 623 | | 326 | 140 | 420 | 2830 |

Figure 3.7: (Left) Occupancy and (Right) Vacancy histogram of SPN-43 aggregated across all channels with observed SPN-43 emissions in San Diego. (Bottom) Summary statistics.

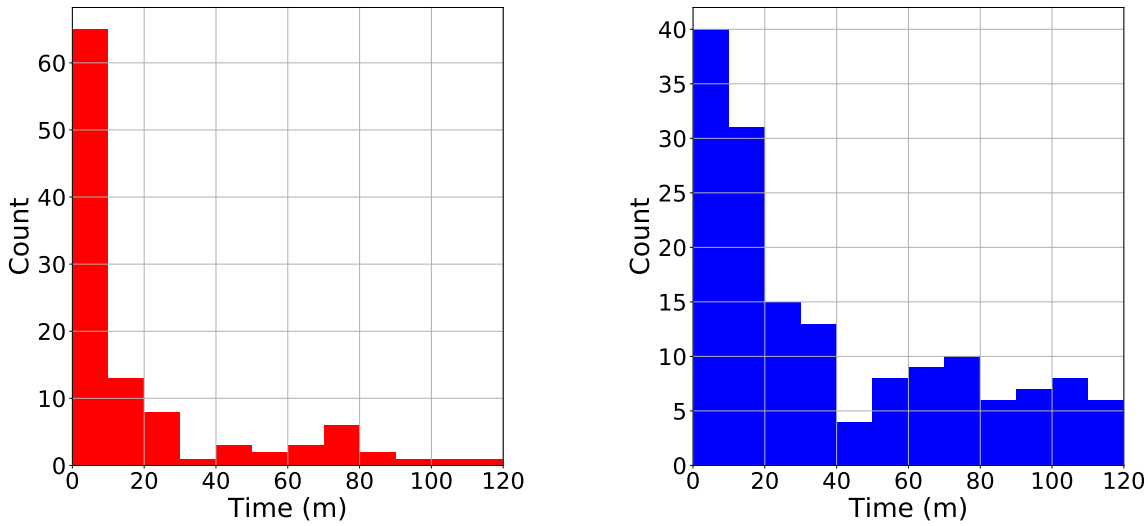


| Type | Total | Occupancy Ratio | $>$ 120 min | Median (min) | 75th Pct (min) | 99th Pct (min) |
|---|---|---|---|---|---|---|
| Occupancy | 133 | $0.092 \pm 0.002$ | 27 | 20 | 80 | 1570 |
| Vacancy | 322 | | 165 | 140 | 430 | 5300 |

Figure 3.8: (Left) Occupancy and (Right) Vacancy histogram of SPN-43 aggregated across all channels with observed SPN-43 emissions in Virginia Beach. (Bottom) Summary statistics.

# Chapter 4

# Results: Ambient Power Distributions

For every multiple of 10 MHz over the entire frequency range observed in San Diego and Virginia Beach (3440-3670 MHz), this chapter presents empirical distributions of the ambient, i.e. SPN-43 absent, peak-detected power spectral density. Namely, for each measurement site with observations at the stated frequency, the empirical CCDF, equal to one minus the CDF, for the power spectral density (in units of dBm/MHz) over a 220 kHz frequency bin is plotted on a semi-log scale. Note that the markers (triangles and circles) on the plots distinguish the two measurement locations, and are spaced uniformly.

The CCDF plots are useful for understanding the upper tails of each distribution. For example, the 90th and 99th percentiles correspond to the power density values where the CCDF is equal to 0.1 and 0.01, respectively. Below the CCDF plots is a table listing estimates for the 50th, 75th, 90th, 95th, and 99th percentiles, organized by antenna type and measurement location. Note that the cavity-backed spiral antenna is abbreviated as CBS and that the omni-directional antenna is abbreviated as Omni.

Uncertainty in each CCDF estimate is indicated by a simultaneous 95% confidence band, shown with dashed lines; see Section 2.4 for details on how this band was estimated. Uncertainties in percentile estimates are communicated with 95% confidence intervals, shown in square brackets to the right of each percentile estimate. As stated in Section 2.4, the percentile confidence intervals were obtained from the simultaneous CCDF confidence band. Therefore, simultaneous inferences involving multiple percentiles can be made at the 5% significance level using these intervals.

As explained in Section 2.1, the spectrograms were collected with various receiver noise floors, due to the changes in the reference level and (site-specific) front-end. To aid in the interpretation of the CCDF plots, tables are given that list the number of spectrograms at each reference level used to estimate a given CDF. The tables are arranged by measurement site and antenna type. The

reference-level counts, together with Table 2.1, indicate the proportion of captures collected at each reference level and their associated noise floor. These proportions are helpful when interpreting the roll-off of empirical CCDFs, since the roll-off corresponds to the noise floor of the observations.

To provide an overview of the results in this chapter, the next two pages present summary plots of the 90th, 95th, and 99th percentiles for the ambient power density distribution at each frequency.

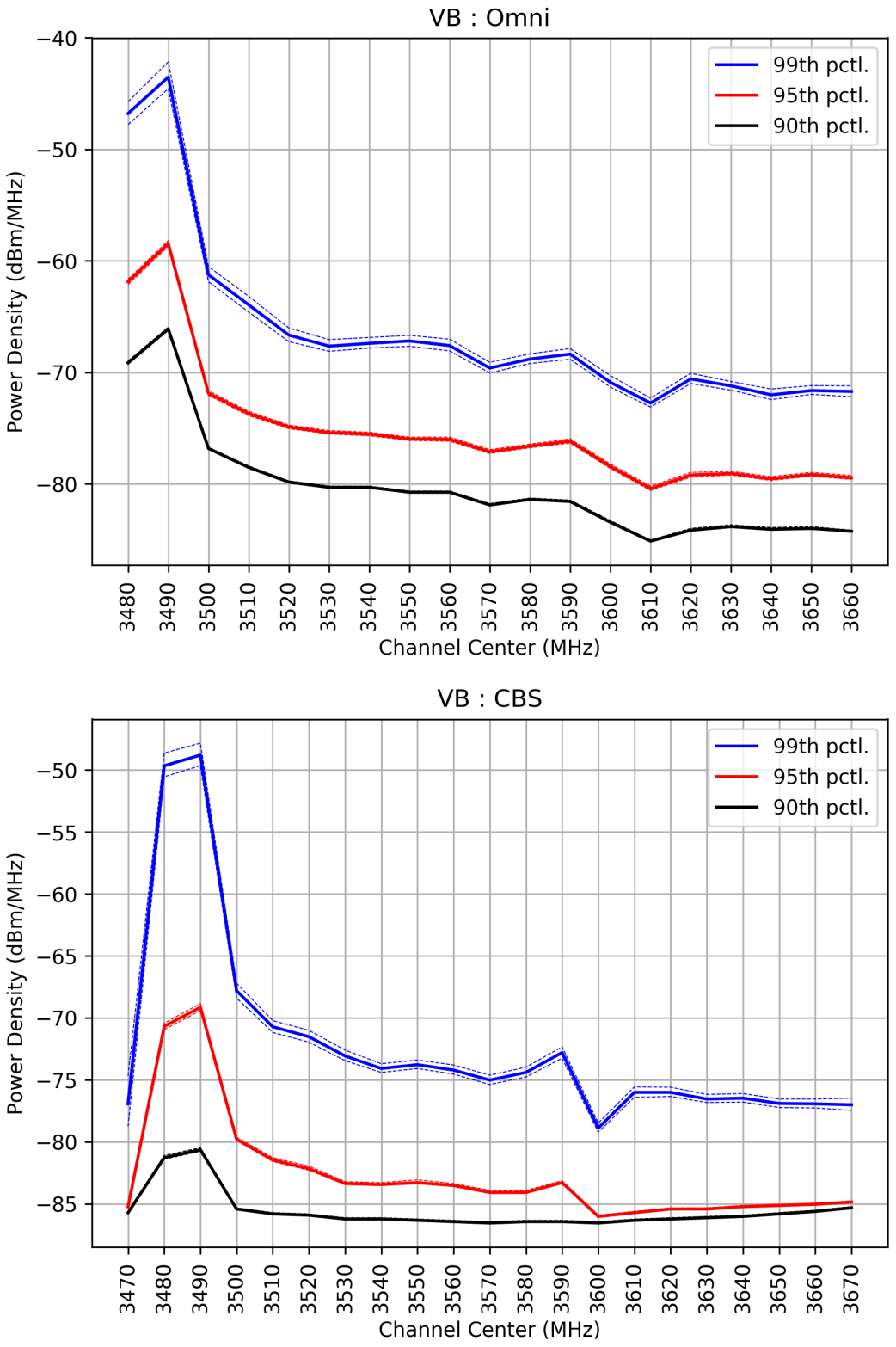


Figure 4.1: Summary of the 90th, 95th, and 99th percentiles for the ambient power density distributions in Virginia Beach. Pointwise 95% confidence bands are indicated by dashed lines.

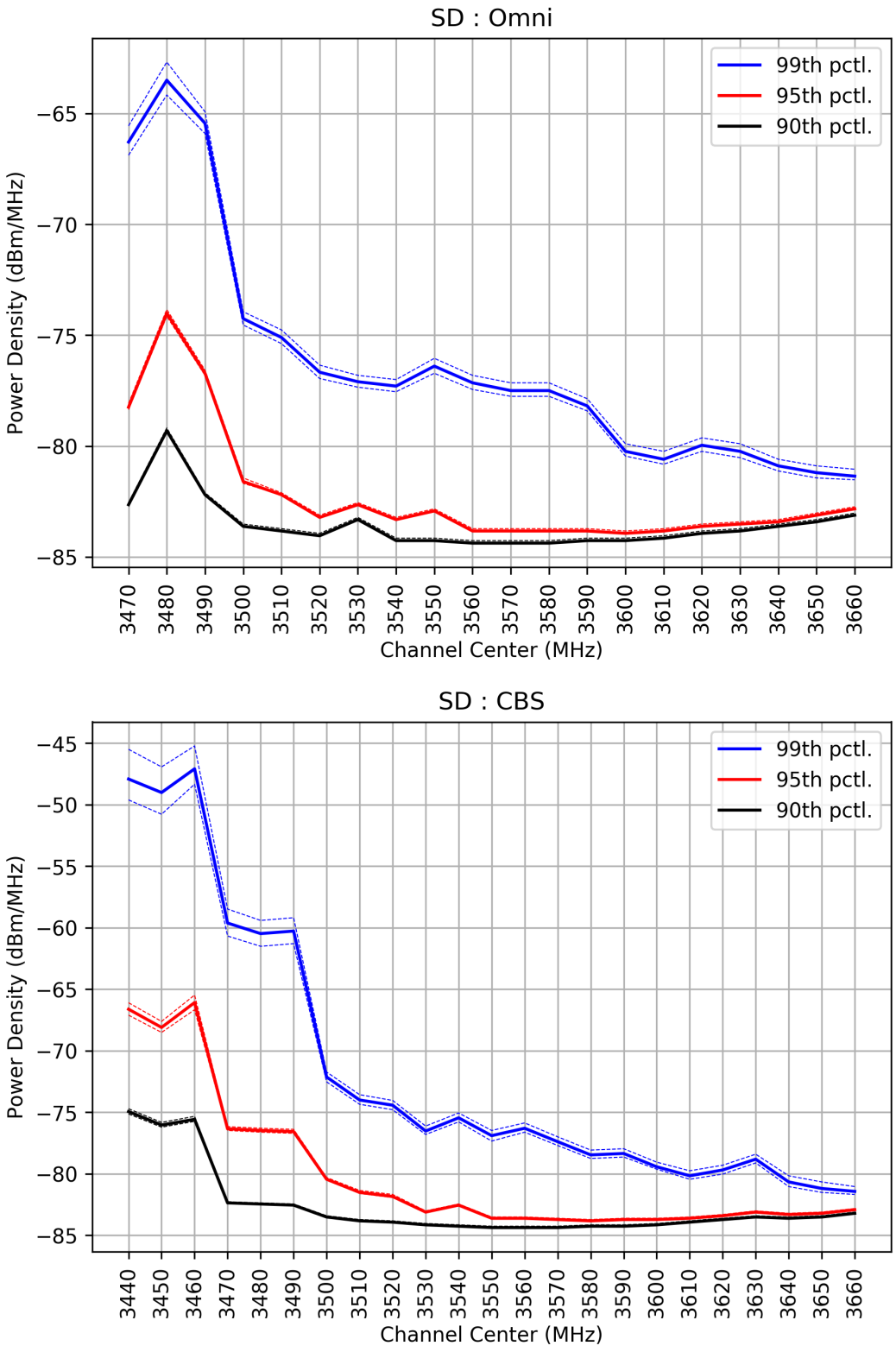


Figure 4.2: Summary of the 90th, 95th, and 99th percentiles for the ambient power density distributions in San Diego. Pointwise 95% confidence bands are indicated by dashed lines.

| Band (MHz) | -30 dB | -20 dB | -10 dB | 0 dB | 5 dB |
|---|---|---|---|---|---|
| 3470 | 0 | 0 | 115 | 2 | 0 |
| 3480 | 432 | 0 | 222 | 2 | 3623 |
| 3490 | 422 | 0 | 202 | 2 | 3611 |
| 3500 | 457 | 0 | 224 | 2 | 3673 |
| 3510 | 457 | 0 | 228 | 6 | 3598 |
| 3520 | 391 | 0 | 203 | 6 | 3674 |
| 3530 | 458 | 0 | 225 | 6 | 3666 |
| 3540 | 463 | 0 | 226 | 6 | 3676 |
| 3550 | 375 | 0 | 194 | 5 | 3676 |
| 3560 | 452 | 0 | 227 | 5 | 3675 |
| 3570 | 299 | 0 | 170 | 3 | 3438 |
| 3580 | 471 | 0 | 230 | 5 | 3685 |
| 3590 | 455 | 0 | 224 | 5 | 3681 |
| 3600 | 459 | 0 | 230 | 6 | 3075 |
| 3610 | 390 | 0 | 194 | 6 | 3676 |
| 3620 | 462 | 0 | 228 | 6 | 3674 |
| 3630 | 456 | 0 | 229 | 5 | 3467 |
| 3640 | 441 | 0 | 216 | 5 | 3683 |
| 3650 | 296 | 0 | 154 | 5 | 3682 |
| 3660 | 451 | 0 | 226 | 5 | 3685 |
| 3670 | 29 | 0 | 2 | 0 | 3660 |

Table 4.1: The number of spectrograms used to calculate the CDFs per band and reference level in Virginia Beach with the CBS antenna.

| Band (MHz) | -30 dB | -20 dB | -10 dB | 0 dB | 5 dB |
|---|---|---|---|---|---|
| 3480 | 0 | 0 | 0 | 497 | 1265 |
| 3490 | 0 | 0 | 0 | 496 | 1248 |
| 3500 | 0 | 0 | 0 | 495 | 1294 |
| 3510 | 0 | 0 | 0 | 499 | 1290 |
| 3520 | 0 | 0 | 0 | 496 | 1282 |
| 3530 | 0 | 0 | 0 | 496 | 1293 |
| 3540 | 0 | 0 | 0 | 489 | 1287 |
| 3550 | 0 | 0 | 0 | 500 | 1288 |
| 3560 | 0 | 0 | 0 | 494 | 1266 |
| 3570 | 0 | 0 | 0 | 447 | 1095 |
| 3580 | 0 | 0 | 0 | 501 | 1296 |
| 3590 | 0 | 0 | 0 | 500 | 1278 |
| 3600 | 0 | 0 | 0 | 392 | 1276 |
| 3610 | 0 | 0 | 0 | 499 | 1293 |
| 3620 | 0 | 0 | 0 | 499 | 1285 |
| 3630 | 0 | 0 | 0 | 501 | 1264 |
| 3640 | 0 | 0 | 0 | 501 | 1289 |
| 3650 | 0 | 0 | 0 | 499 | 1280 |
| 3660 | 0 | 0 | 0 | 498 | 1284 |

Table 4.2: The number of spectrograms used to calculate the CDFs per band and reference level in Virginia Beach with the Omni antenna.

| Band (MHz) | -30 dB | -20 dB | -10 dB | 0 dB | 5 dB |
|---|---|---|---|---|---|
| 3440 | 0 | 0 | 0 | 0 | 657 |
| 3450 | 0 | 0 | 0 | 0 | 780 |
| 3460 | 0 | 0 | 0 | 0 | 796 |
| 3470 | 479 | 1 | 1 | 0 | 2965 |
| 3480 | 435 | 1 | 1 | 0 | 2883 |
| 3490 | 426 | 1 | 1 | 0 | 2938 |
| 3500 | 358 | 1 | 1 | 0 | 2976 |
| 3510 | 475 | 1 | 1 | 0 | 2984 |
| 3520 | 485 | 1 | 1 | 0 | 2735 |
| 3530 | 492 | 1 | 1 | 0 | 2959 |
| 3540 | 476 | 1 | 1 | 0 | 2983 |
| 3550 | 192 | 1 | 1 | 0 | 2248 |
| 3560 | 475 | 1 | 1 | 0 | 2983 |
| 3570 | 467 | 1 | 1 | 0 | 2978 |
| 3580 | 458 | 1 | 1 | 0 | 2946 |
| 3590 | 489 | 1 | 1 | 0 | 2988 |
| 3600 | 488 | 1 | 1 | 0 | 2879 |
| 3610 | 468 | 1 | 1 | 0 | 2983 |
| 3620 | 435 | 0 | 1 | 0 | 2983 |
| 3630 | 400 | 1 | 1 | 0 | 2985 |
| 3640 | 486 | 1 | 1 | 0 | 2308 |
| 3650 | 483 | 1 | 1 | 0 | 2177 |
| 3660 | 410 | 1 | 1 | 0 | 2172 |

Table 4.3: The number of spectrograms used to calculate the CDFs per band and reference level in San Diego with the CBS antenna.

| Band (MHz) | -30 dB | -20 dB | -10 dB | 0 dB | 5 dB |
|---|---|---|---|---|---|
| 3470 | 0 | 0 | 0 | 0 | 4548 |
| 3480 | 0 | 0 | 0 | 0 | 3277 |
| 3490 | 0 | 0 | 0 | 0 | 4636 |
| 3500 | 0 | 0 | 0 | 0 | 4667 |
| 3510 | 0 | 0 | 0 | 0 | 4689 |
| 3520 | 0 | 0 | 0 | 0 | 4673 |
| 3530 | 0 | 0 | 0 | 0 | 4619 |
| 3540 | 0 | 0 | 0 | 0 | 4689 |
| 3550 | 0 | 0 | 0 | 0 | 3455 |
| 3560 | 0 | 0 | 0 | 0 | 4710 |
| 3570 | 0 | 0 | 0 | 0 | 4736 |
| 3580 | 0 | 0 | 0 | 0 | 4705 |
| 3590 | 0 | 0 | 0 | 0 | 4698 |
| 3600 | 0 | 0 | 0 | 0 | 4693 |
| 3610 | 0 | 0 | 0 | 0 | 4737 |
| 3620 | 0 | 0 | 0 | 0 | 4713 |
| 3630 | 0 | 0 | 0 | 0 | 4713 |
| 3640 | 0 | 0 | 0 | 0 | 4731 |
| 3650 | 0 | 0 | 0 | 0 | 4741 |
| 3660 | 0 | 0 | 0 | 0 | 4731 |

Table 4.4: The number of spectrograms used to calculate the CDFs per band and reference level in San Diego with the Omni antenna.

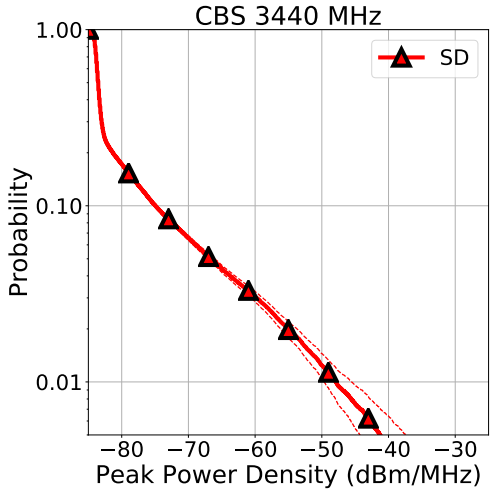


| Antenna | Location | Count | Percentile | Estimate (dBm/MHz) |
|---|---|---|---|---|
| CBS | SD | 657 | 50th | -83.5, [-83.5, -83.4] |
| | | | 75th | -82.6, [-82.6, -82.5] |
| | | | 90th | -74.9, [-75.1, -74.7] |
| | | | 95th | -66.6, [-67.1, -66.1] |
| | | | 99th | -47.9, [-49.6, -45.5] |

Figure 4.3: CCDFs of 3440 MHz band when SPN-43 is not present and table for each antenna type including 95% non-parametric confidence bounds denoted by dashed lines. Table contains quantile information with 95% confidence intervals in square brackets.

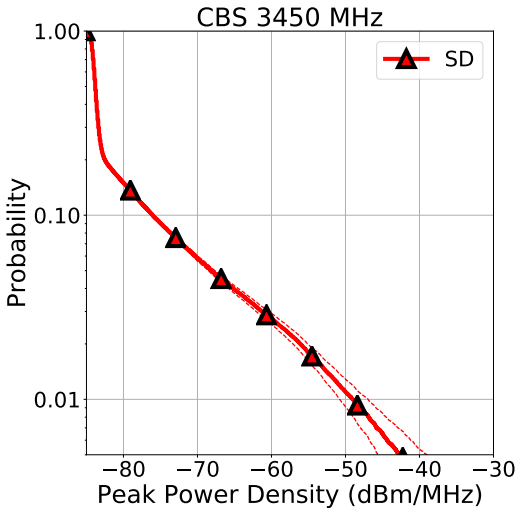


| Antenna | Location | Count | Percentile | Estimate (dBm/MHz) |
|---|---|---|---|---|
| CBS | SD | 780 | 50th | -83.8, [-83.8, -83.7] |
| | | | 75th | -83.1, [-83.1, -83.0] |
| | | | 90th | -76.0, [-76.2, -75.8] |
| | | | 95th | -68.1, [-68.5, -67.6] |
| | | | 99th | -49.0, [-50.8, -46.9] |

Figure 4.4: CCDFs of 3450 MHz band when SPN-43 is not present and table for each antenna type including 95% non-parametric confidence bounds denoted by dashed lines. Table contains quantile information with 95% confidence intervals in square brackets.

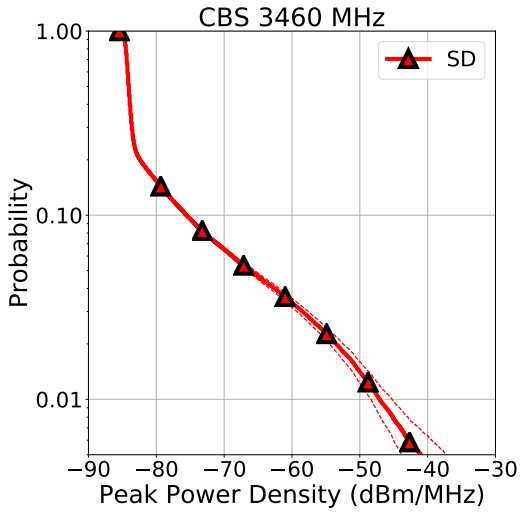


| Antenna | Location | Count | Percentile | Estimate (dBm/MHz) |
|---|---|---|---|---|
| CBS | SD | 796 | 50th | -84.0, [-84.0, -83.9] |
| | | | 75th | -83.3, [-83.3, -83.2] |
| | | | 90th | -75.6, [-75.8, -75.3] |
| | | | 95th | -66.1, [-66.7, -65.5] |
| | | | 99th | -47.1, [-48.4, -45.2] |

Figure 4.5: CCDFs of 3460 MHz band when SPN-43 is not present and table for each antenna type including 95% non-parametric confidence bounds denoted by dashed lines. Table contains quantile information with 95% confidence intervals in square brackets.

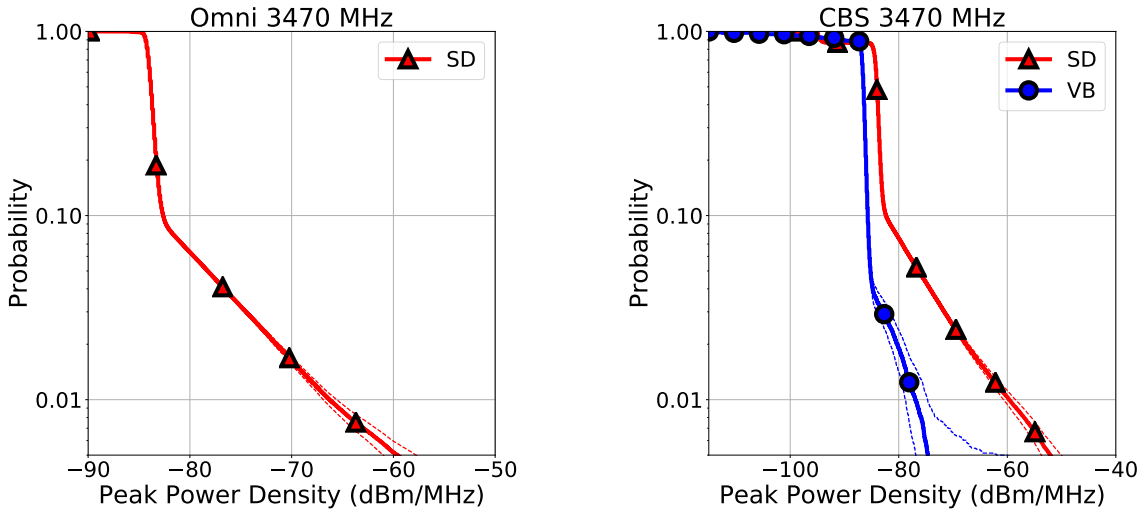


| Antenna | Location | Count | Percentile | Estimate (dBm/MHz) |
|---|---|---|---|---|
| Omni | SD | 4,548 | 50th | -83.8, [-83.8, -83.7] |
| | | | 75th | -83.4, [-83.4, -83.3] |
| | | | 90th | -82.6, [-82.6, -82.5] |
| | | | 95th | -78.2, [-78.4, -78.1] |
| | | | 99th | -66.3, [-66.9, -65.6] |
| CBS | SD | 3,446 | 50th | -84.0, [-84.0, -83.9] |
| | | | 75th | -83.5, [-83.5, -83.4] |
| | | | 90th | -82.4, [-82.4, -82.3] |
| | | | 95th | -76.3, [-76.5, -76.2] |
| | | | 99th | -59.6, [-60.7, -58.5] |
| | VB | 117 | 50th | -86.6, [-86.6, -86.5] |
| | | | 75th | -86.1, [-86.1, -86.0] |
| | | | 90th | -85.7, [-85.7, -85.6] |
| | | | 95th | -85.2, [-85.3, -85.0] |
| | | | 99th | -76.9, [-78.8, -74.7] |

Figure 4.6: CCDFs of 3470 MHz band when SPN-43 is not present and table for each antenna type including 95% non-parametric confidence bounds denoted by dashed lines. Table contains quantile information with 95% confidence intervals in square brackets.

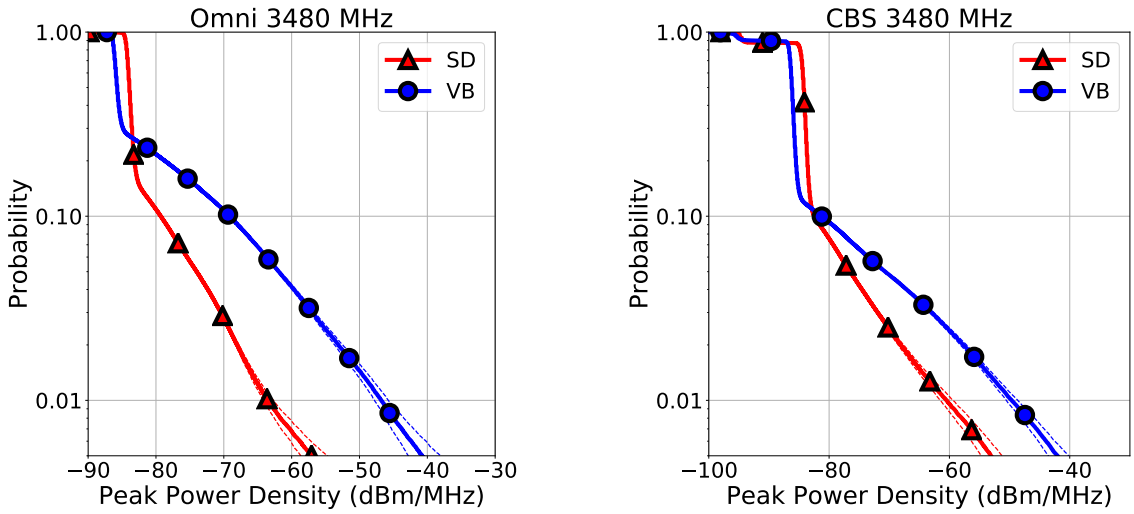


| Antenna | Location | Count | Percentile | Estimate (dBm/MHz) |
|---|---|---|---|---|
| Omni | SD | 3,277 | 50th | -83.9, [-83.9, -83.8] |
| | | | 75th | -83.4, [-83.4, -83.3] |
| | | | 90th | -79.3, [-79.4, -79.2] |
| | | | 95th | -74.0, [-74.2, -73.8] |
| | | | 99th | -63.5, [-64.2, -62.7] |
| | VB | 1,762 | 50th | -85.7, [-85.7, -85.6] |
| | | | 75th | -82.3, [-82.4, -82.2] |
| | | | 90th | -69.1, [-69.3, -69.0] |
| | | | 95th | -61.9, [-62.1, -61.6] |
| | | | 99th | -46.8, [-47.8, -45.8] |
| CBS | SD | 3,320 | 50th | -84.3, [-84.3, -84.2] |
| | | | 75th | -83.7, [-83.7, -83.6] |
| | | | 90th | -82.5, [-82.5, -82.4] |
| | | | 95th | -76.5, [-76.6, -76.3] |
| | | | 99th | -60.5, [-61.5, -59.4] |
| | VB | 4,279 | 50th | -86.2, [-86.2, -86.1] |
| | | | 75th | -85.7, [-85.7, -85.6] |
| | | | 90th | -81.3, [-81.4, -81.1] |
| | | | 95th | -70.7, [-70.9, -70.4] |
| | | | 99th | -49.7, [-50.5, -48.6] |

Figure 4.7: CCDFs of 3480 MHz band when SPN-43 is not present and table for each antenna type including 95% non-parametric confidence bounds denoted by dashed lines. Table contains quantile information with 95% confidence intervals in square brackets.

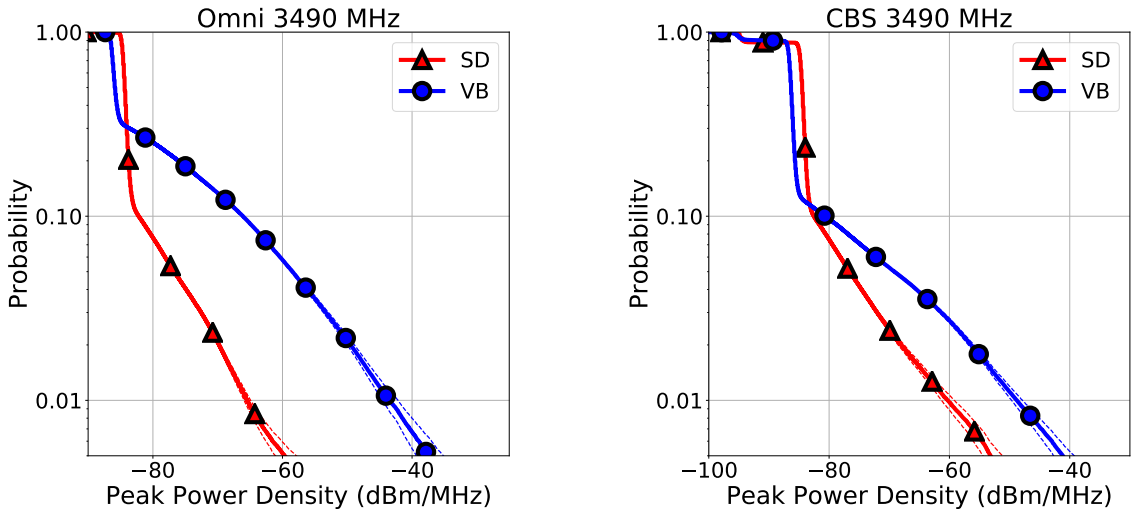


| Antenna | Location | Count | Percentile | Estimate (dBm/MHz) |
|---|---|---|---|---|
| Omni | SD | 4,636 | 50th | -84.4, [-84.4, -84.3] |
| | | | 75th | -83.9, [-83.9, -83.8] |
| | | | 90th | -82.2, [-82.2, -82.1] |
| | | | 95th | -76.7, [-76.8, -76.6] |
| | | | 99th | -65.4, [-65.9, -64.9] |
| | VB | 1,744 | 50th | -85.9, [-85.9, -85.8] |
| | | | 75th | -79.9, [-80.0, -79.8] |
| | | | 90th | -66.1, [-66.2, -66.0] |
| | | | 95th | -58.5, [-58.7, -58.2] |
| | | | 99th | -43.5, [-44.6, -42.2] |
| CBS | SD | 3,366 | 50th | -84.5, [-84.5, -84.4] |
| | | | 75th | -84.0, [-84.0, -83.9] |
| | | | 90th | -82.6, [-82.5, -82.5] |
| | | | 95th | -76.6, [-76.7, -76.4] |
| | | | 99th | -60.3, [-61.3, -59.2] |
| | VB | 4,237 | 50th | -86.3, [-86.3, -86.2] |
| | | | 75th | -85.8, [-85.8, -85.7] |
| | | | 90th | -80.6, [-80.8, -80.5] |
| | | | 95th | -69.1, [-69.4, -68.9] |
| | | | 99th | -48.8, [-49.6, -47.8] |

Figure 4.8: CCDFs of 3490 MHz band when SPN-43 is not present and table for each antenna type including 95% non-parametric confidence bounds denoted by dashed lines. Table contains quantile information with 95% confidence intervals in square brackets.

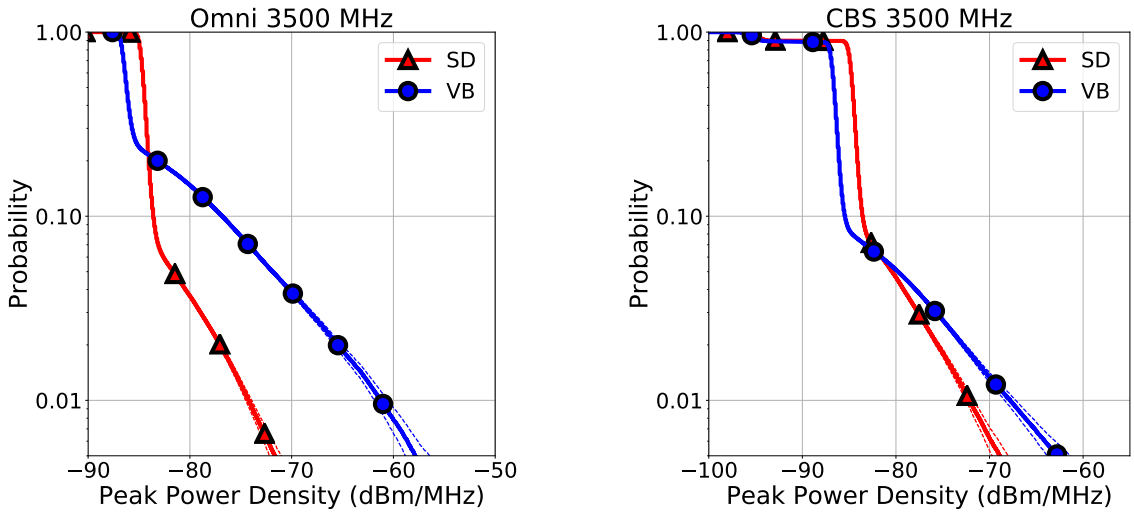


| Antenna | Location | Count | Percentile | Estimate (dBm/MHz) |
|---|---|---|---|---|
| Omni | SD | 4,667 | 50th | -84.5, [-84.5, -84.4] |
| | | | 75th | -84.2, [-84.2, -84.0] |
| | | | 90th | -83.6, [-83.6, -83.5] |
| | | | 95th | -81.6, [-81.7, -81.4] |
| | | | 99th | -74.3, [-74.5, -73.9] |
| | VB | 1,789 | 50th | -86.2, [-86.2, -86.1] |
| | | | 75th | -85.2, [-85.2, -85.1] |
| | | | 90th | -76.8, [-76.9, -76.7] |
| | | | 95th | -71.9, [-72.1, -71.7] |
| | | | 99th | -61.3, [-61.9, -60.5] |
| CBS | SD | 3,336 | 50th | -84.6, [-84.6, -84.5] |
| | | | 75th | -84.3, [-84.3, -84.2] |
| | | | 90th | -83.5, [-83.5, -83.4] |
| | | | 95th | -80.5, [-80.5, -80.3] |
| | | | 99th | -72.1, [-72.5, -71.7] |
| | VB | 4,356 | 50th | -86.7, [-86.7, -86.5] |
| | | | 75th | -86.2, [-86.2, -86.1] |
| | | | 90th | -85.4, [-85.4, -85.3] |
| | | | 95th | -79.8, [-79.9, -79.6] |
| | | | 99th | -67.8, [-68.4, -67.2] |

Figure 4.9: CCDFs of 3500 MHz band when SPN-43 is not present and table for each antenna type including 95% non-parametric confidence bounds denoted by dashed lines. Table contains quantile information with 95% confidence intervals in square brackets.

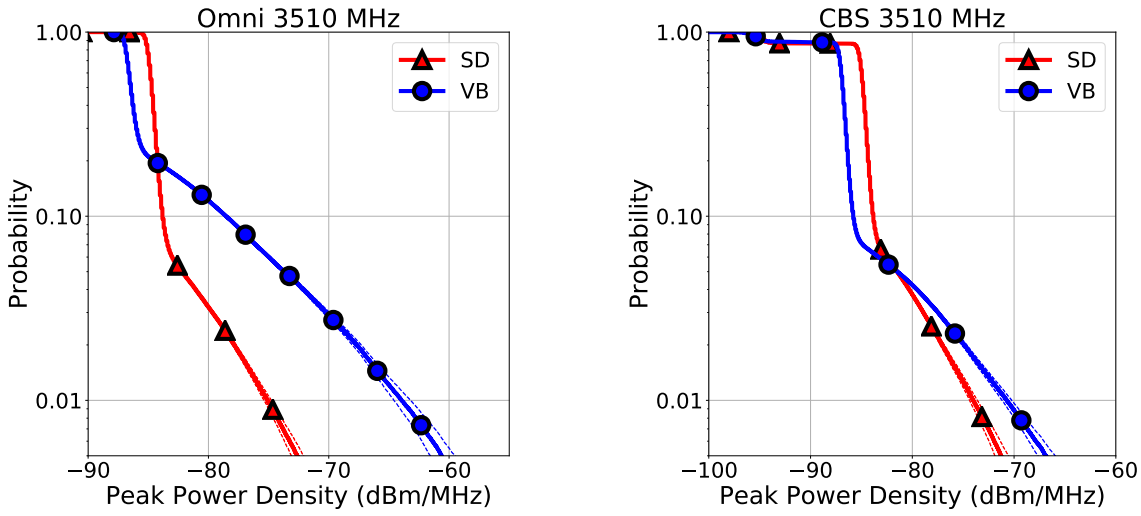


| Antenna | Location | Count | Percentile | Estimate (dBm/MHz) |
|---|---|---|---|---|
| Omni | SD | 4,689 | 50th | -84.7, [-84.7, -84.6] |
| | | | 75th | -84.4, [-84.4, -84.3] |
| | | | 90th | -83.8, [-83.8, -83.7] |
| | | | 95th | -82.2, [-82.2, -82.1] |
| | | | 99th | -75.1, [-75.4, -74.8] |
| | VB | 1,789 | 50th | -86.4, [-86.4, -86.3] |
| | | | 75th | -85.7, [-85.7, -85.6] |
| | | | 90th | -78.5, [-78.6, -78.4] |
| | | | 95th | -73.7, [-73.9, -73.5] |
| | | | 99th | -64.0, [-64.6, -63.2] |
| CBS | SD | 3,461 | 50th | -84.8, [-84.8, -84.7] |
| | | | 75th | -84.5, [-84.5, -84.4] |
| | | | 90th | -83.8, [-83.8, -83.7] |
| | | | 95th | -81.5, [-81.6, -81.4] |
| | | | 99th | -74.0, [-74.4, -73.6] |
| | VB | 4,289 | 50th | -86.9, [-86.9, -86.8] |
| | | | 75th | -86.4, [-86.4, -86.3] |
| | | | 90th | -85.8, [-85.8, -85.7] |
| | | | 95th | -81.5, [-81.6, -81.3] |
| | | | 99th | -70.7, [-71.2, -70.2] |

Figure 4.10: CCDFs of 3510 MHz band when SPN-43 is not present and table for each antenna type including 95% non-parametric confidence bounds denoted by dashed lines. Table contains quantile information with 95% confidence intervals in square brackets.

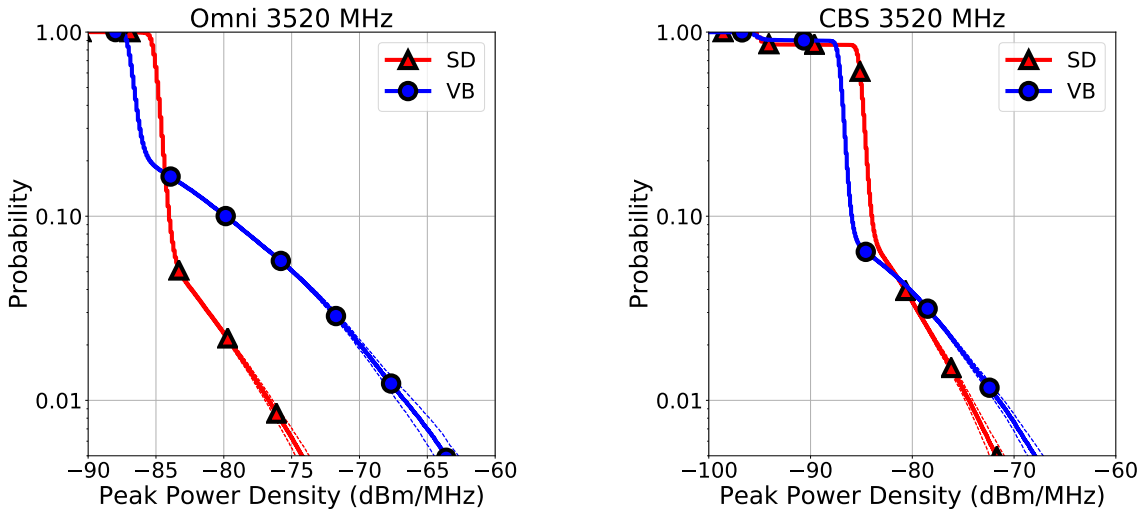


| Antenna | Location | Count | Percentile | Estimate (dBm/MHz) |
|---|---|---|---|---|
| Omni | SD | 4,673 | 50th | -84.8, [-84.8, -84.7] |
| | | | 75th | -84.5, [-84.5, -84.4] |
| | | | 90th | -84.0, [-84.0, -83.9] |
| | | | 95th | -83.2, [-83.2, -83.1] |
| | | | 99th | -76.7, [-77.0, -76.3] |
| | VB | 1,778 | 50th | -86.7, [-86.7, -86.5] |
| | | | 75th | -85.9, [-85.9, -85.8] |
| | | | 90th | -79.8, [-79.9, -79.8] |
| | | | 95th | -74.9, [-75.0, -74.7] |
| | | | 99th | -66.7, [-67.2, -66.0] |
| CBS | SD | 3,222 | 50th | -85.0, [-85.0, -84.8] |
| | | | 75th | -84.6, [-84.6, -84.5] |
| | | | 90th | -83.9, [-83.9, -83.8] |
| | | | 95th | -81.8, [-81.9, -81.7] |
| | | | 99th | -74.4, [-74.8, -74.0] |
| | VB | 4,274 | 50th | -87.0, [-87.0, -86.9] |
| | | | 75th | -86.6, [-86.5, -86.4] |
| | | | 90th | -85.9, [-85.9, -85.8] |
| | | | 95th | -82.2, [-82.3, -82.0] |
| | | | 99th | -71.5, [-72.0, -71.0] |

Figure 4.11: CCDFs of 3520 MHz band when SPN-43 is not present and table for each antenna type including 95% non-parametric confidence bounds denoted by dashed lines. Table contains quantile information with 95% confidence intervals in square brackets.

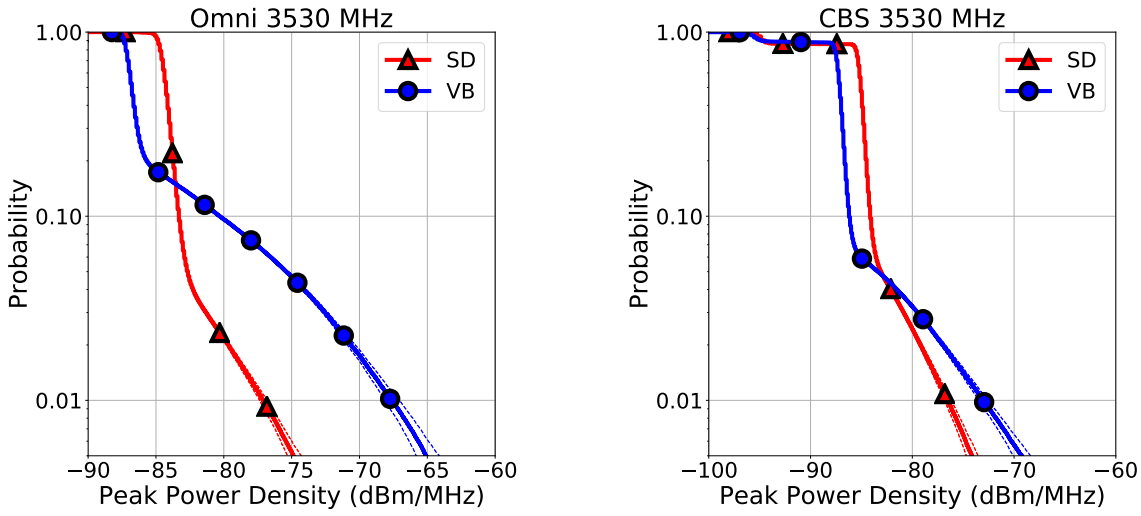


| Antenna | Location | Count | Percentile | Estimate (dBm/MHz) |
|---|---|---|---|---|
| Omni | SD | 4,619 | 50th | -84.3, [-84.3, -84.2] |
| | | | 75th | -83.8, [-83.8, -83.7] |
| | | | 90th | -83.3, [-83.3, -83.2] |
| | | | 95th | -82.6, [-82.6, -82.5] |
| | | | 99th | -77.1, [-77.3, -76.8] |
| | VB | 1,789 | 50th | -86.8, [-86.8, -86.7] |
| | | | 75th | -86.1, [-86.1, -86.0] |
| | | | 90th | -80.3, [-80.4, -80.2] |
| | | | 95th | -75.4, [-75.5, -75.2] |
| | | | 99th | -67.7, [-68.1, -67.1] |
| CBS | SD | 3,453 | 50th | -85.1, [-85.1, -85.0] |
| | | | 75th | -84.6, [-84.6, -84.5] |
| | | | 90th | -84.2, [-84.2, -84.0] |
| | | | 95th | -83.1, [-83.1, -83.0] |
| | | | 99th | -76.5, [-76.8, -76.1] |
| | VB | 4,355 | 50th | -87.1, [-87.1, -87.0] |
| | | | 75th | -86.8, [-86.8, -86.7] |
| | | | 90th | -86.2, [-86.2, -86.1] |
| | | | 95th | -83.4, [-83.4, -83.2] |
| | | | 99th | -73.1, [-73.5, -72.6] |

Figure 4.12: CCDFs of 3530 MHz band when SPN-43 is not present and table for each antenna type including 95% non-parametric confidence bounds denoted by dashed lines. Table contains quantile information with 95% confidence intervals in square brackets.

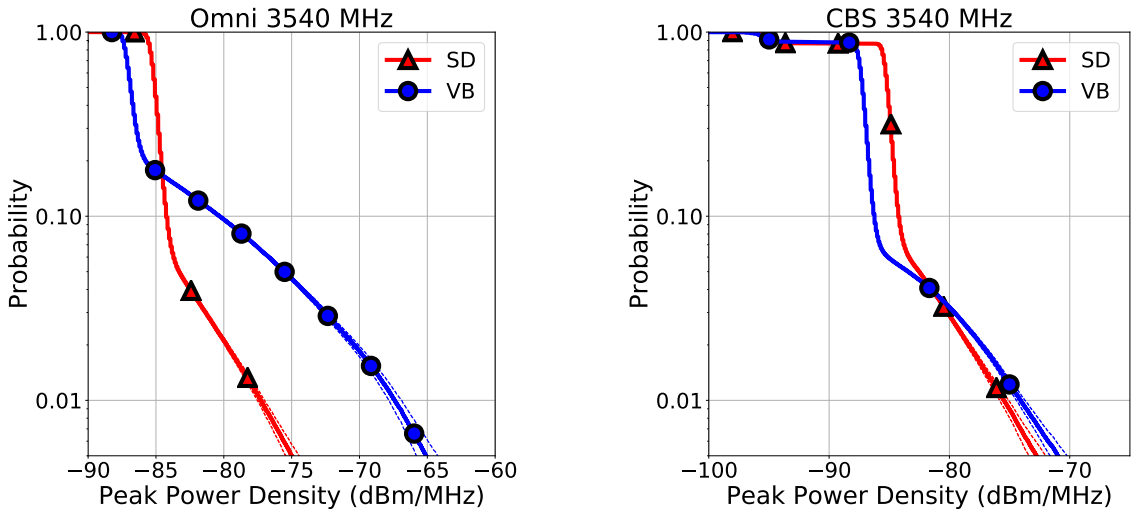


| Antenna | Location | Count | Percentile | Estimate (dBm/MHz) |
|---|---|---|---|---|
| Omni | SD | 4,689 | 50th | -85.1, [-85.1, -85.0] |
| | | | 75th | -84.7, [-84.7, -84.6] |
| | | | 90th | -84.3, [-84.3, -84.2] |
| | | | 95th | -83.3, [-83.3, -83.2] |
| | | | 99th | -77.3, [-77.5, -77.0] |
| | VB | 1,776 | 50th | -86.9, [-86.9, -86.8] |
| | | | 75th | -86.2, [-86.2, -86.1] |
| | | | 90th | -80.3, [-80.4, -80.2] |
| | | | 95th | -75.5, [-75.7, -75.4] |
| | | | 99th | -67.4, [-67.8, -66.9] |
| CBS | SD | 3,461 | 50th | -85.2, [-85.2, -85.1] |
| | | | 75th | -84.7, [-84.7, -84.6] |
| | | | 90th | -84.3, [-84.3, -84.2] |
| | | | 95th | -82.6, [-82.5, -82.5] |
| | | | 99th | -75.5, [-75.8, -75.1] |
| | VB | 4,371 | 50th | -87.2, [-87.2, -87.1] |
| | | | 75th | -86.8, [-86.8, -86.7] |
| | | | 90th | -86.2, [-86.2, -86.1] |
| | | | 95th | -83.4, [-83.5, -83.3] |
| | | | 99th | -74.1, [-74.4, -73.7] |

Figure 4.13: CCDFs of 3540 MHz band when SPN-43 is not present and table for each antenna type including 95% non-parametric confidence bounds denoted by dashed lines. Table contains quantile information with 95% confidence intervals in square brackets.

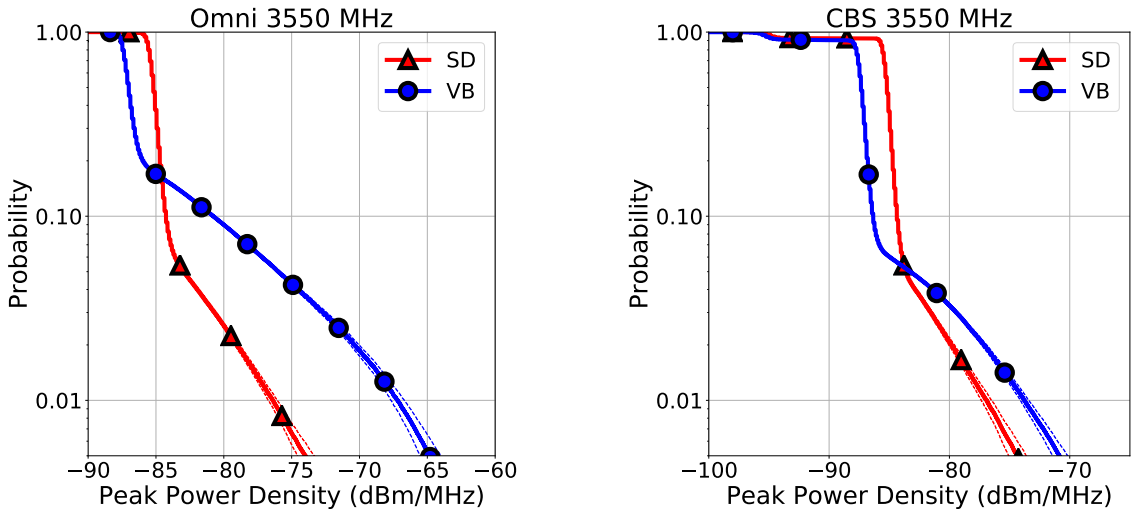


| Antenna | Location | Count | Percentile | Estimate (dBm/MHz) |
|---|---|---|---|---|
| Omni | SD | 3,455 | 50th | -85.2, [-85.2, -85.1] |
| | | | 75th | -84.8, [-84.8, -84.7] |
| | | | 90th | -84.3, [-84.3, -84.2] |
| | | | 95th | -82.9, [-82.9, -82.8] |
| | | | 99th | -76.4, [-76.7, -76.0] |
| | VB | 1,788 | 50th | -87.0, [-87.0, -86.9] |
| | | | 75th | -86.4, [-86.4, -86.3] |
| | | | 90th | -80.8, [-80.8, -80.6] |
| | | | 95th | -76.0, [-76.1, -75.8] |
| | | | 99th | -67.2, [-67.7, -66.7] |
| CBS | SD | 2,442 | 50th | -85.2, [-85.2, -85.1] |
| | | | 75th | -84.8, [-84.8, -84.7] |
| | | | 90th | -84.4, [-84.4, -84.3] |
| | | | 95th | -83.6, [-83.6, -83.5] |
| | | | 99th | -76.9, [-77.3, -76.5] |
| | VB | 4,250 | 50th | -87.4, [-87.4, -87.2] |
| | | | 75th | -86.9, [-86.9, -86.8] |
| | | | 90th | -86.3, [-86.3, -86.2] |
| | | | 95th | -83.3, [-83.4, -83.1] |
| | | | 99th | -73.8, [-74.1, -73.4] |

Figure 4.14: CCDFs of 3550 MHz band when SPN-43 is not present and table for each antenna type including 95% non-parametric confidence bounds denoted by dashed lines. Table contains quantile information with 95% confidence intervals in square brackets.

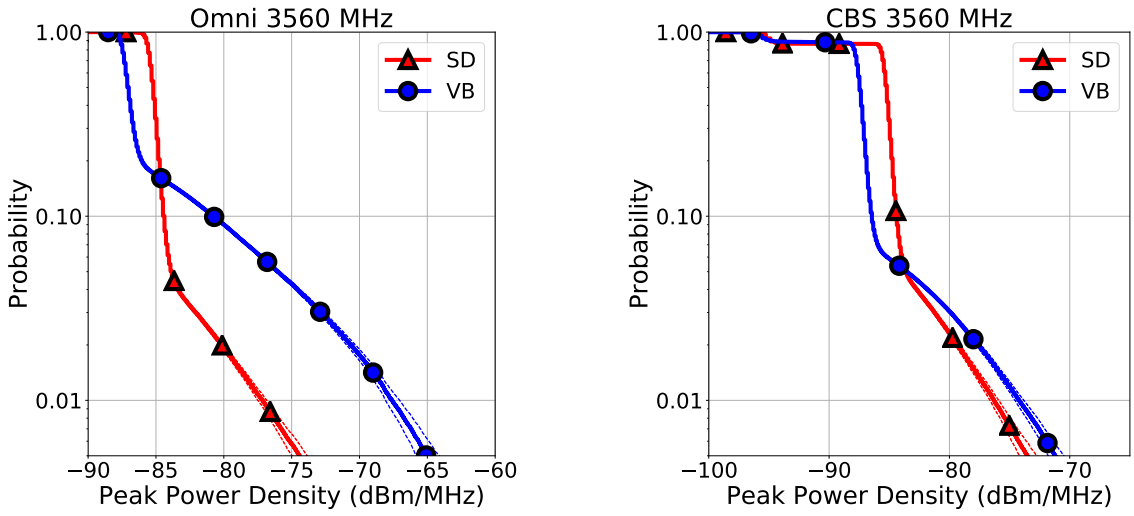


| Antenna | Location | Count | Percentile | Estimate (dBm/MHz) |
|---|---|---|---|---|
| Omni | SD | 4,710 | 50th | -85.2, [-85.2, -85.1] |
| | | | 75th | -84.8, [-84.8, -84.7] |
| | | | 90th | -84.4, [-84.4, -84.3] |
| | | | 95th | -83.8, [-83.8, -83.7] |
| | | | 99th | -77.1, [-77.5, -76.8] |
| | VB | 1,760 | 50th | -87.0, [-87.0, -86.9] |
| | | | 75th | -86.4, [-86.4, -86.3] |
| | | | 90th | -80.8, [-80.8, -80.6] |
| | | | 95th | -76.0, [-76.2, -75.8] |
| | | | 99th | -67.6, [-68.1, -67.0] |
| CBS | SD | 3,460 | 50th | -85.2, [-85.2, -85.1] |
| | | | 75th | -84.8, [-84.8, -84.7] |
| | | | 90th | -84.4, [-84.4, -84.3] |
| | | | 95th | -83.6, [-83.6, -83.5] |
| | | | 99th | -76.3, [-76.6, -75.9] |
| | VB | 4,359 | 50th | -87.5, [-87.5, -87.4] |
| | | | 75th | -87.0, [-87.0, -86.9] |
| | | | 90th | -86.4, [-86.4, -86.3] |
| | | | 95th | -83.5, [-83.6, -83.4] |
| | | | 99th | -74.2, [-74.5, -73.8] |

Figure 4.15: CCDFs of 3560 MHz band when SPN-43 is not present and table for each antenna type including 95% non-parametric confidence bounds denoted by dashed lines. Table contains quantile information with 95% confidence intervals in square brackets.

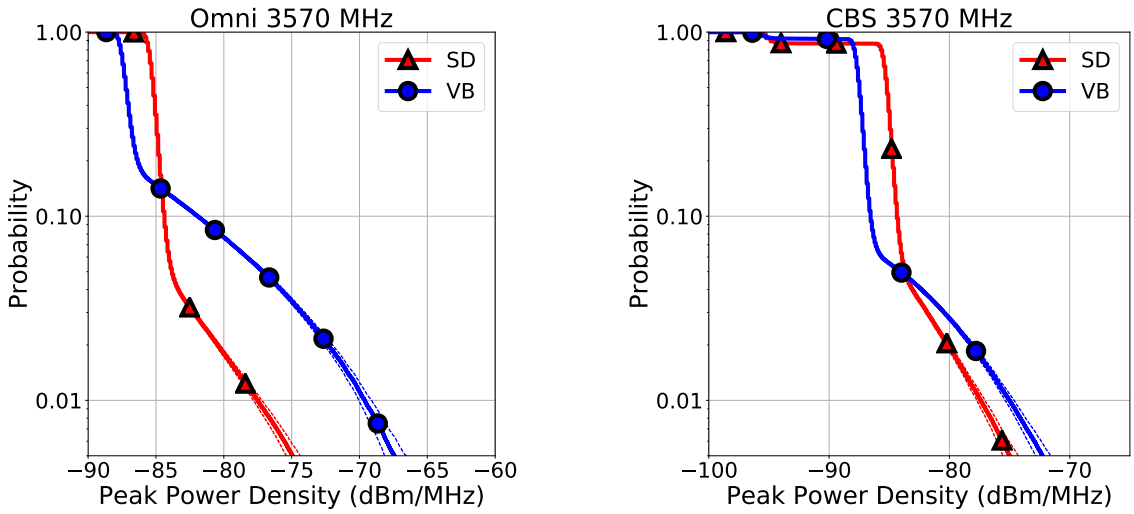


| Antenna | Location | Count | Percentile | Estimate (dBm/MHz) |
|---|---|---|---|---|
| Omni | SD | 4,736 | 50th | -85.2, [-85.2, -85.1] |
| | | | 75th | -84.8, [-84.8, -84.7] |
| | | | 90th | -84.4, [-84.4, -84.3] |
| | | | 95th | -83.8, [-83.8, -83.7] |
| | | | 99th | -77.5, [-77.8, -77.2] |
| | VB | 1,542 | 50th | -87.2, [-87.2, -87.1] |
| | | | 75th | -86.7, [-86.7, -86.5] |
| | | | 90th | -81.9, [-82.0, -81.8] |
| | | | 95th | -77.1, [-77.3, -76.9] |
| | | | 99th | -69.6, [-70.0, -69.1] |
| CBS | SD | 3,447 | 50th | -85.2, [-85.2, -85.1] |
| | | | 75th | -84.8, [-84.8, -84.7] |
| | | | 90th | -84.4, [-84.4, -84.3] |
| | | | 95th | -83.7, [-83.7, -83.6] |
| | | | 99th | -77.4, [-77.7, -77.0] |
| | VB | 3,910 | 50th | -87.5, [-87.5, -87.4] |
| | | | 75th | -87.1, [-87.1, -87.0] |
| | | | 90th | -86.6, [-86.5, -86.4] |
| | | | 95th | -84.1, [-84.2, -83.9] |
| | | | 99th | -75.0, [-75.4, -74.6] |

Figure 4.16: CCDFs of 3570 MHz band when SPN-43 is not present and table for each antenna type including 95% non-parametric confidence bounds denoted by dashed lines. Table contains quantile information with 95% confidence intervals in square brackets.

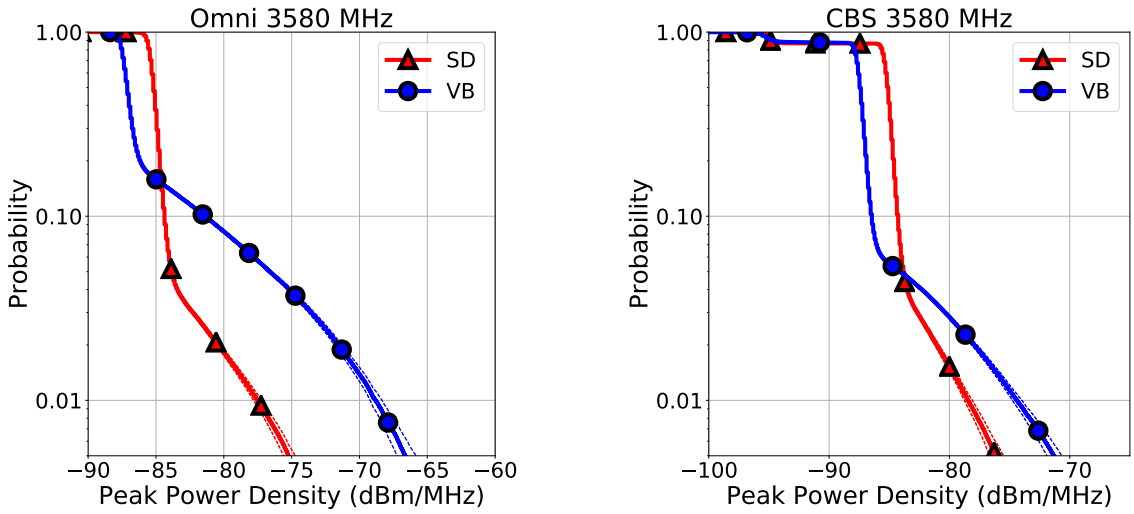


| Antenna | Location | Count | Percentile | Estimate (dBm/MHz) |
|---|---|---|---|---|
| Omni | SD | 4,705 | 50th | -85.2, [-85.2, -85.1] |
| | | | 75th | -84.8, [-84.8, -84.7] |
| | | | 90th | -84.4, [-84.4, -84.3] |
| | | | 95th | -83.8, [-83.8, -83.7] |
| | | | 99th | -77.5, [-77.8, -77.2] |
| | VB | 1,797 | 50th | -87.1, [-87.1, -87.0] |
| | | | 75th | -86.6, [-86.5, -86.4] |
| | | | 90th | -81.4, [-81.5, -81.3] |
| | | | 95th | -76.6, [-76.8, -76.4] |
| | | | 99th | -68.8, [-69.2, -68.3] |
| CBS | SD | 3,406 | 50th | -85.1, [-85.1, -85.0] |
| | | | 75th | -84.7, [-84.7, -84.6] |
| | | | 90th | -84.3, [-84.3, -84.2] |
| | | | 95th | -83.8, [-83.8, -83.7] |
| | | | 99th | -78.5, [-78.8, -78.1] |
| | VB | 4,391 | 50th | -87.5, [-87.5, -87.4] |
| | | | 75th | -87.0, [-87.0, -86.9] |
| | | | 90th | -86.4, [-86.4, -86.3] |
| | | | 95th | -84.1, [-84.2, -83.9] |
| | | | 99th | -74.4, [-74.8, -74.0] |

Figure 4.17: CCDFs of 3580 MHz band when SPN-43 is not present and table for each antenna type including 95% non-parametric confidence bounds denoted by dashed lines. Table contains quantile information with 95% confidence intervals in square brackets.

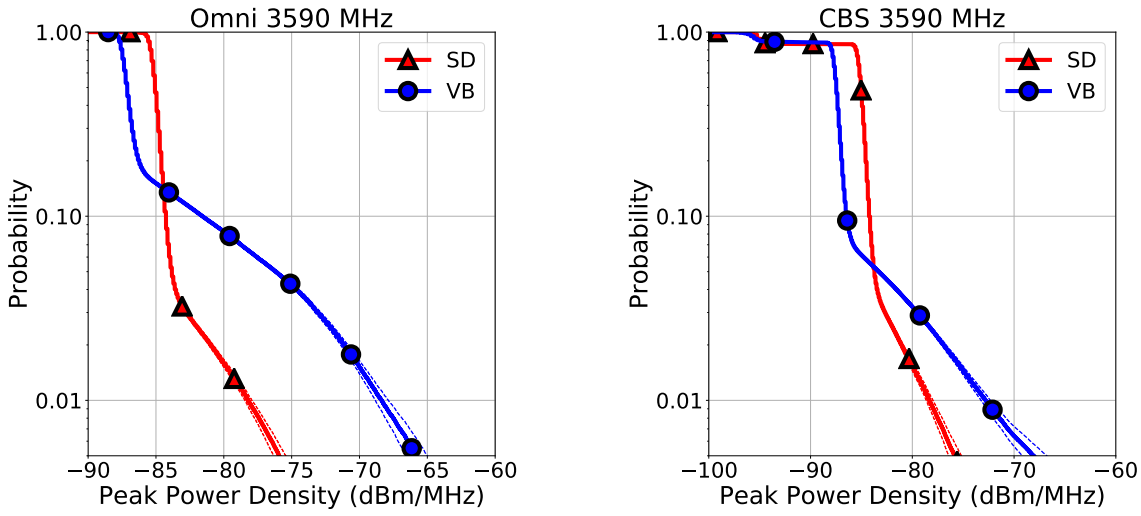


| Antenna | Location | Count | Percentile | Estimate (dBm/MHz) |
|---|---|---|---|---|
| Omni | SD | 4,698 | 50th | -85.1, [-85.1, -85.0] |
| | | | 75th | -84.7, [-84.7, -84.6] |
| | | | 90th | -84.3, [-84.3, -84.2] |
| | | | 95th | -83.8, [-83.8, -83.7] |
| | | | 99th | -78.2, [-78.4, -77.9] |
| | VB | 1,778 | 50th | -87.1, [-87.1, -87.0] |
| | | | 75th | -86.6, [-86.5, -86.4] |
| | | | 90th | -81.6, [-81.7, -81.5] |
| | | | 95th | -76.2, [-76.3, -76.0] |
| | | | 99th | -68.4, [-68.8, -67.9] |
| CBS | SD | 3,479 | 50th | -85.1, [-85.1, -85.0] |
| | | | 75th | -84.6, [-84.6, -84.5] |
| | | | 90th | -84.3, [-84.3, -84.2] |
| | | | 95th | -83.7, [-83.7, -83.6] |
| | | | 99th | -78.4, [-78.6, -78.0] |
| | VB | 4,365 | 50th | -87.5, [-87.5, -87.4] |
| | | | 75th | -87.1, [-87.1, -87.0] |
| | | | 90th | -86.4, [-86.4, -86.3] |
| | | | 95th | -83.3, [-83.4, -83.1] |
| | | | 99th | -72.8, [-73.3, -72.3] |

Figure 4.18: CCDFs of 3590 MHz band when SPN-43 is not present and table for each antenna type including 95% non-parametric confidence bounds denoted by dashed lines. Table contains quantile information with 95% confidence intervals in square brackets.

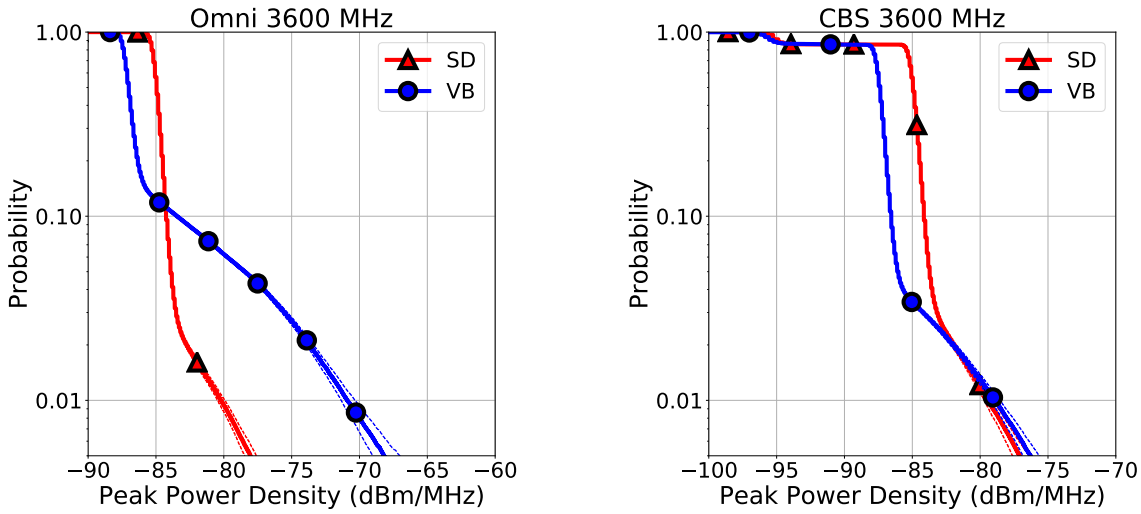


| Antenna | Location | Count | Percentile | Estimate (dBm/MHz) |
|---|---|---|---|---|
| Omni | SD | 4,693 | 50th | -85.0, [-85.0, -84.8] |
| | | | 75th | -84.6, [-84.6, -84.5] |
| | | | 90th | -84.3, [-84.3, -84.2] |
| | | | 95th | -83.9, [-83.9, -83.8] |
| | | | 99th | -80.2, [-80.5, -79.9] |
| | VB | 1,668 | 50th | -87.0, [-87.0, -86.9] |
| | | | 75th | -86.6, [-86.5, -86.4] |
| | | | 90th | -83.4, [-83.5, -83.3] |
| | | | 95th | -78.4, [-78.6, -78.2] |
| | | | 99th | -70.9, [-71.3, -70.3] |
| CBS | SD | 3,369 | 50th | -85.0, [-85.0, -84.8] |
| | | | 75th | -84.6, [-84.6, -84.5] |
| | | | 90th | -84.2, [-84.2, -84.0] |
| | | | 95th | -83.7, [-83.7, -83.6] |
| | | | 99th | -79.4, [-79.6, -79.1] |
| | VB | 3,770 | 50th | -87.4, [-87.4, -87.2] |
| | | | 75th | -87.0, [-87.0, -86.9] |
| | | | 90th | -86.6, [-86.5, -86.4] |
| | | | 95th | -86.0, [-86.0, -85.9] |
| | | | 99th | -78.9, [-79.2, -78.5] |

Figure 4.19: CCDFs of 3600 MHz band when SPN-43 is not present and table for each antenna type including 95% non-parametric confidence bounds denoted by dashed lines. Table contains quantile information with 95% confidence intervals in square brackets.

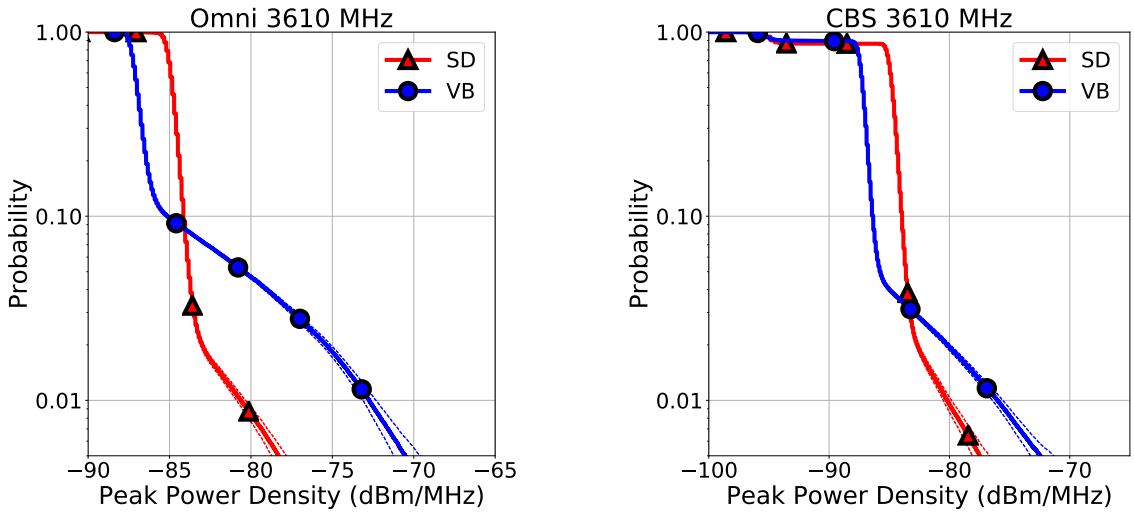


| Antenna | Location | Count | Percentile | Estimate (dBm/MHz) |
|---|---|---|---|---|
| Omni | SD | 4,737 | 50th | -84.8, [-84.8, -84.7] |
| | | | 75th | -84.5, [-84.5, -84.4] |
| | | | 90th | -84.2, [-84.2, -84.0] |
| | | | 95th | -83.8, [-83.8, -83.7] |
| | | | 99th | -80.6, [-80.8, -80.2] |
| | VB | 1,792 | 50th | -87.0, [-87.0, -86.9] |
| | | | 75th | -86.6, [-86.5, -86.4] |
| | | | 90th | -85.1, [-85.1, -85.0] |
| | | | 95th | -80.4, [-80.6, -80.2] |
| | | | 99th | -72.8, [-73.1, -72.3] |
| CBS | SD | 3,453 | 50th | -84.7, [-84.7, -84.6] |
| | | | 75th | -84.4, [-84.4, -84.3] |
| | | | 90th | -83.9, [-83.9, -83.8] |
| | | | 95th | -83.6, [-83.6, -83.5] |
| | | | 99th | -80.2, [-80.5, -79.8] |
| | VB | 4,266 | 50th | -87.2, [-87.2, -87.1] |
| | | | 75th | -86.9, [-86.9, -86.8] |
| | | | 90th | -86.3, [-86.3, -86.2] |
| | | | 95th | -85.7, [-85.7, -85.6] |
| | | | 99th | -76.0, [-76.4, -75.6] |

Figure 4.20: CCDFs of 3610 MHz band when SPN-43 is not present and table for each antenna type including 95% non-parametric confidence bounds denoted by dashed lines. Table contains quantile information with 95% confidence intervals in square brackets.

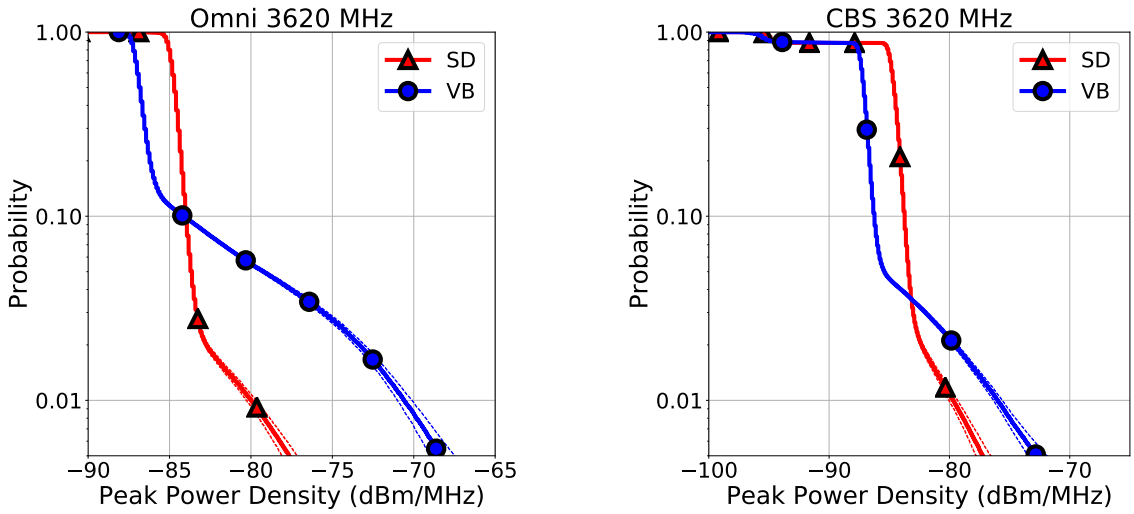


| Antenna | Location | Count | Percentile | Estimate (dBm/MHz) |
|---|---|---|---|---|
| Omni | SD | 4,713 | 50th | -84.7, [-84.7, -84.6] |
| | | | 75th | -84.4, [-84.4, -84.3] |
| | | | 90th | -83.9, [-83.9, -83.8] |
| | | | 95th | -83.6, [-83.6, -83.5] |
| | | | 99th | -80.0, [-80.2, -79.6] |
| | VB | 1,784 | 50th | -86.8, [-86.8, -86.7] |
| | | | 75th | -86.3, [-86.3, -86.2] |
| | | | 90th | -84.2, [-84.2, -84.0] |
| | | | 95th | -79.2, [-79.4, -79.0] |
| | | | 99th | -70.6, [-71.0, -70.1] |
| CBS | SD | 3,419 | 50th | -84.6, [-84.6, -84.5] |
| | | | 75th | -84.2, [-84.2, -84.0] |
| | | | 90th | -83.7, [-83.7, -83.6] |
| | | | 95th | -83.4, [-83.4, -83.3] |
| | | | 99th | -79.7, [-80.0, -79.3] |
| | VB | 4,370 | 50th | -87.1, [-87.1, -87.0] |
| | | | 75th | -86.8, [-86.8, -86.7] |
| | | | 90th | -86.2, [-86.2, -86.1] |
| | | | 95th | -85.4, [-85.4, -85.3] |
| | | | 99th | -76.0, [-76.3, -75.6] |

Figure 4.21: CCDFs of 3620 MHz band when SPN-43 is not present and table for each antenna type including 95% non-parametric confidence bounds denoted by dashed lines. Table contains quantile information with 95% confidence intervals in square brackets.

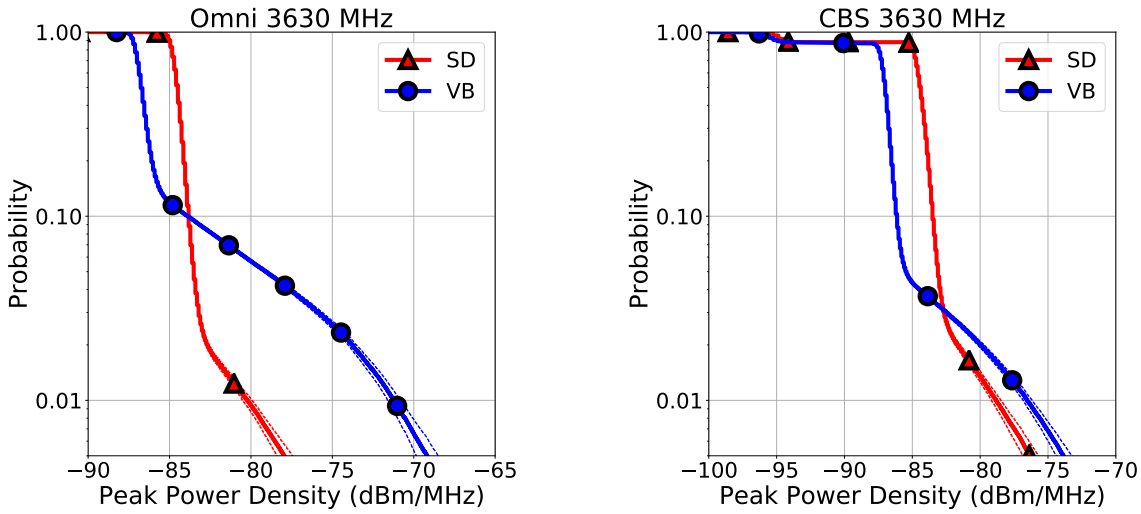


| Antenna | Location | Count | Percentile | Estimate (dBm/MHz) |
|---|---|---|---|---|
| Omni | SD | 4,713 | 50th | -84.5, [-84.5, -84.4] |
| | | | 75th | -84.2, [-84.2, -84.0] |
| | | | 90th | -83.8, [-83.8, -83.7] |
| | | | 95th | -83.5, [-83.5, -83.4] |
| | | | 99th | -80.2, [-80.5, -79.9] |
| | VB | 1,765 | 50th | -86.8, [-86.8, -86.7] |
| | | | 75th | -86.2, [-86.2, -86.1] |
| | | | 90th | -83.8, [-83.9, -83.7] |
| | | | 95th | -79.1, [-79.2, -78.9] |
| | | | 99th | -71.2, [-71.6, -70.8] |
| CBS | SD | 3,387 | 50th | -84.4, [-84.4, -84.3] |
| | | | 75th | -83.9, [-83.9, -83.8] |
| | | | 90th | -83.5, [-83.5, -83.4] |
| | | | 95th | -83.1, [-83.1, -83.0] |
| | | | 99th | -78.8, [-79.1, -78.4] |
| | VB | 4,157 | 50th | -87.0, [-87.0, -86.9] |
| | | | 75th | -86.7, [-86.7, -86.5] |
| | | | 90th | -86.1, [-86.1, -86.0] |
| | | | 95th | -85.4, [-85.4, -85.3] |
| | | | 99th | -76.5, [-76.8, -76.2] |

Figure 4.22: CCDFs of 3630 MHz band when SPN-43 is not present and table for each antenna type including 95% non-parametric confidence bounds denoted by dashed lines. Table contains quantile information with 95% confidence intervals in square brackets.

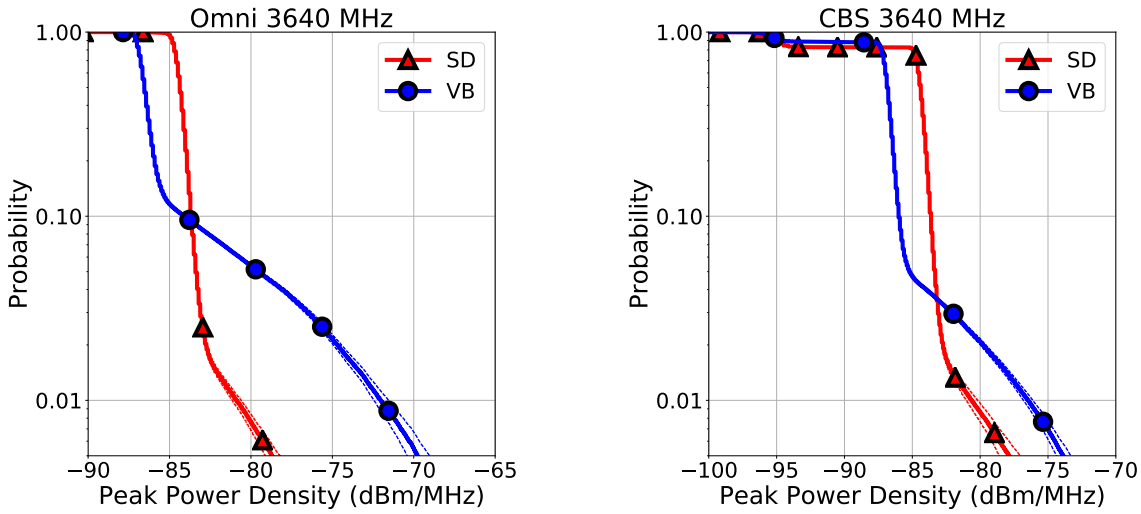


| Antenna | Location | Count | Percentile | Estimate (dBm/MHz) |
|---|---|---|---|---|
| Omni | SD | 4,731 | 50th | -84.4, [-84.4, -84.3] |
| | | | 75th | -84.0, [-84.0, -83.9] |
| | | | 90th | -83.6, [-83.6, -83.5] |
| | | | 95th | -83.4, [-83.4, -83.3] |
| | | | 99th | -80.9, [-81.1, -80.6] |
| | VB | 1,790 | 50th | -86.6, [-86.5, -86.4] |
| | | | 75th | -86.1, [-86.1, -86.0] |
| | | | 90th | -84.1, [-84.1, -83.9] |
| | | | 95th | -79.5, [-79.7, -79.3] |
| | | | 99th | -72.0, [-72.4, -71.5] |
| CBS | SD | 2,796 | 50th | -84.4, [-84.4, -84.3] |
| | | | 75th | -84.0, [-84.0, -83.9] |
| | | | 90th | -83.6, [-83.6, -83.5] |
| | | | 95th | -83.3, [-83.3, -83.2] |
| | | | 99th | -80.7, [-81.0, -80.2] |
| | VB | 4,345 | 50th | -86.9, [-86.9, -86.8] |
| | | | 75th | -86.4, [-86.4, -86.3] |
| | | | 90th | -86.0, [-86.0, -85.9] |
| | | | 95th | -85.2, [-85.2, -85.1] |
| | | | 99th | -76.5, [-76.8, -76.1] |

Figure 4.23: CCDFs of 3640 MHz band when SPN-43 is not present and table for each antenna type including 95% non-parametric confidence bounds denoted by dashed lines. Table contains quantile information with 95% confidence intervals in square brackets.

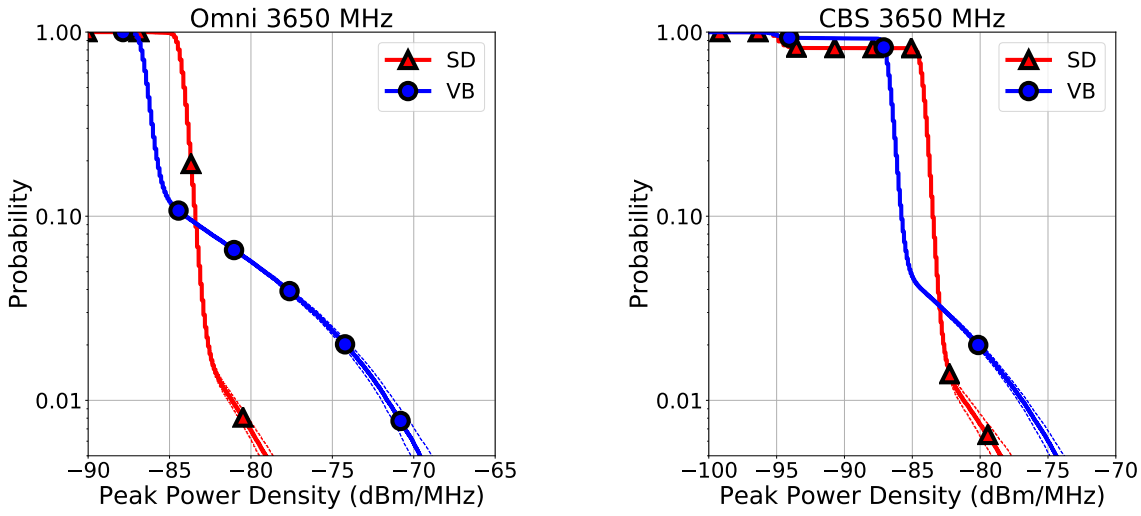


| Antenna | Location | Count | Percentile | Estimate (dBm/MHz) |
|---|---|---|---|---|
| Omni | SD | 4,741 | 50th | -84.2, [-84.2, -84.0] |
| | | | 75th | -83.8, [-83.8, -83.7] |
| | | | 90th | -83.4, [-83.4, -83.3] |
| | | | 95th | -83.1, [-83.1, -83.0] |
| | | | 99th | -81.2, [-81.4, -80.9] |
| | VB | 1,779 | 50th | -86.3, [-86.3, -86.2] |
| | | | 75th | -85.9, [-85.9, -85.8] |
| | | | 90th | -84.0, [-84.1, -83.8] |
| | | | 95th | -79.2, [-79.3, -79.0] |
| | | | 99th | -71.6, [-72.0, -71.2] |
| CBS | SD | 2,662 | 50th | -84.2, [-84.2, -84.0] |
| | | | 75th | -83.8, [-83.8, -83.7] |
| | | | 90th | -83.5, [-83.5, -83.4] |
| | | | 95th | -83.2, [-83.2, -83.1] |
| | | | 99th | -81.2, [-81.5, -80.7] |
| | VB | 4,137 | 50th | -86.7, [-86.7, -86.5] |
| | | | 75th | -86.2, [-86.2, -86.1] |
| | | | 90th | -85.8, [-85.8, -85.7] |
| | | | 95th | -85.1, [-85.1, -85.0] |
| | | | 99th | -76.9, [-77.2, -76.5] |

Figure 4.24: CCDFs of 3650 MHz band when SPN-43 is not present and table for each antenna type including 95% non-parametric confidence bounds denoted by dashed lines. Table contains quantile information with 95% confidence intervals in square brackets.

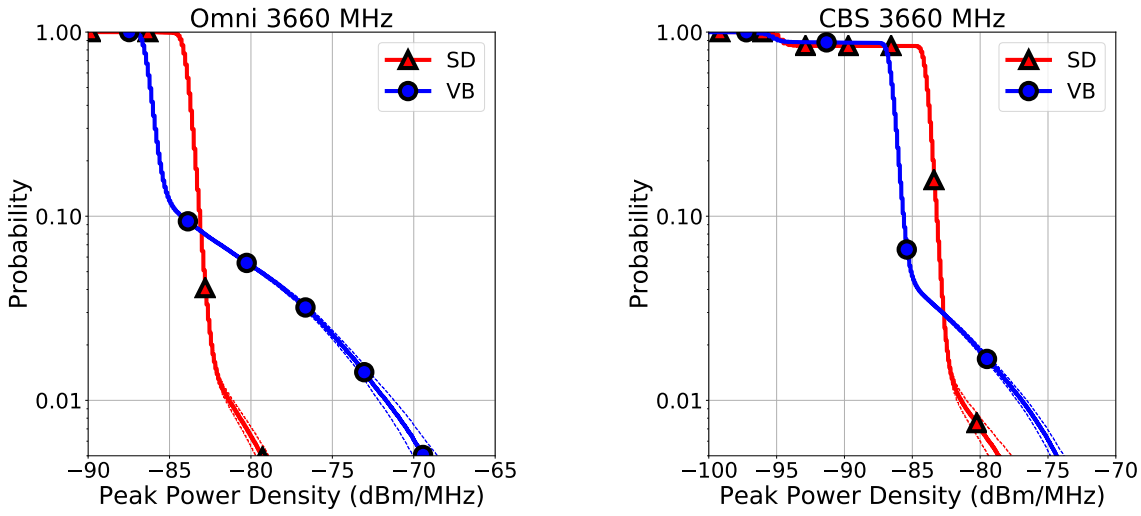


| Antenna | Location | Count | Percentile | Estimate (dBm/MHz) |
|---|---|---|---|---|
| Omni | SD | 4,731 | 50th | -83.8, [-83.8, -83.7] |
| | | | 75th | -83.5, [-83.5, -83.4] |
| | | | 90th | -83.1, [-83.1, -83.0] |
| | | | 95th | -82.8, [-82.8, -82.7] |
| | | | 99th | -81.4, [-81.5, -81.0] |
| | VB | 1,782 | 50th | -86.2, [-86.2, -86.1] |
| | | | 75th | -85.7, [-85.7, -85.6] |
| | | | 90th | -84.2, [-84.2, -84.2] |
| | | | 95th | -79.4, [-79.6, -79.3] |
| | | | 99th | -71.7, [-72.2, -71.2] |
| CBS | SD | 2,584 | 50th | -83.9, [-83.9, -83.8] |
| | | | 75th | -83.5, [-83.5, -83.4] |
| | | | 90th | -83.2, [-83.2, -83.1] |
| | | | 95th | -82.9, [-82.9, -82.8] |
| | | | 99th | -81.4, [-81.7, -81.0] |
| | VB | 4,367 | 50th | -86.4, [-86.4, -86.3] |
| | | | 75th | -86.1, [-86.1, -86.0] |
| | | | 90th | -85.6, [-85.6, -85.5] |
| | | | 95th | -85.0, [-85.0, -85.0] |
| | | | 99th | -76.9, [-77.3, -76.5] |

Figure 4.25: CCDFs of 3660 MHz band when SPN-43 is not present and table for each antenna type including 95% non-parametric confidence bounds denoted by dashed lines. Table contains quantile information with 95% confidence intervals in square brackets.

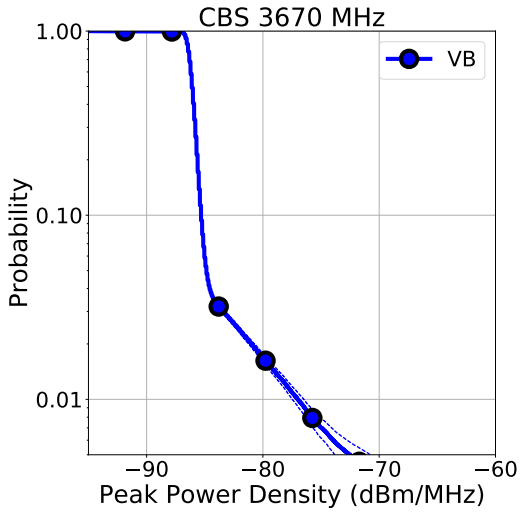


| Antenna | Location | Count | Percentile | Estimate (dBm/MHz) |
|---|---|---|---|---|
| CBS | VB | 3,691 | 50th | -86.1, [-86.1, -86.0] |
| | | | 75th | -85.7, [-85.7, -85.6] |
| | | | 90th | -85.3, [-85.3, -85.2] |
| | | | 95th | -84.9, [-84.9, -84.8] |
| | | | 99th | -77.0, [-77.5, -76.5] |

Figure 4.26: CCDFs of 3670 MHz band when SPN-43 is not present and table for each antenna type including 95% non-parametric confidence bounds denoted by dashed lines. Table contains quantile information with 95% confidence intervals in square brackets.

# Chapter 5

# Summary and Discussion

This report provided empirical distributions for channel occupancy and ambient (SPN-43 absent) power derived from a set of over 14,000 3.5 GHz band spectrograms collected over two-month intervals in both San Diego and Virginia Beach. Channel occupancy distributions were provided for each 10 MHz channel in which SPN-43 emissions were captured. For San Diego, the channels with observed SPN-43 emissions were centered at 3520 MHz, 3550 MHz and 3600 MHz. For Virginia Beach, SPN-43 emissions were observed in channels centered at 3570 MHz, 3600 MHz and 3630 MHz. To supplement the channel occupancy distributions, the occupancy ratio of each band at each measurement site and estimated 50th, 75th and 99th percentiles of both vacancy and occupancy time-intervals were given. In addition, we provided ambient power CCDFs for each multiple of 10 MHz between 3440-3670 MHz. Separate CCDFs were plotted for each antenna type (cavity backed spiral and omni-directional) and measurement location (San Diego and Virginia Beach). Estimates of the 50th, 75th, 90th, 95th, and 99th percentiles for ambient power were included with each CCDF.

The descriptive statistics presented here may be useful to both federal regulators and potential commercial users of the CBRS band. Specifically, the channel occupancy distributions are pertinent to a requirement that a channel be vacated by commercial wireless networks for a specified time-period after detection of an incumbent signal [8]. Also, the occupancy statistics could inform expectations for channel availability. Ambient power distributions are relevant to selection of background noise levels used in ESC certification testing [9]. In addition, the ambient power distributions could help ESC developers choose detection methods that can successfully operate with the observed levels of non-SPN-43 emissions.

As explained in Section 2.2, roughly 30% of the spectrograms were labeled for SPN-43 presence by a human, based on subjective visual interpretation. Note that ship locations or assigned frequencies were not available during or after the measurements. The remaining unlabeled spectrograms were

classified for SPN-43 presence by applying a CNN, as described in [10]. The strong detection performance of the CNN enabled highly-accurate estimation of spectrum occupancy statistics and ambient power distributions. A worse-performing detection method would have resulted in more false-positives and missed detections at a given decision threshold, adding estimation bias to the findings.

Finally, it should be emphasized that the results presented here are based on measurements collected over two-month periods at two geographical locations. Due to the limited nature of these observations, caution should be exercised to not draw overly-general conclusions. In particular, factors such as radar prevalence, ship movements, and radio frequency propagation conditions were uncontrolled and unverified. Therefore, the findings given in this report may not be indicative of the full range or prevalence of emissions present at different times or at other coastal locations.

# Appendix A

# Change Log

Revision 1 - November 19, 2018

- Added paragraph to Section 2.1 discussing the frequency responses of the pre-selector and receiver.
- Revised plots in Chapter 4 to only include results for frequencies in the passband of the pre-selector and receiver.
- Revised all tables in Chapter 4 to correctly reflect the number of spectrograms used for each empirical distribution estimate.
- Added four plots to the beginning of Chapter 4 that summarize the 90th, 95th, and 99th percentiles of the ambient power distribution at each measurement frequency.
- Changed the frequency range covered by the ambient power results to 3440-3670 MHz throughout the document, which required minor edits to the abstract, Chapter 1, Chapter 2, Chapter 4, and Chapter 5.

# Bibliography


[1] "Citizens broadband radio service," Code of Federal Regulations. Title 47, Part 96, June 2015.

[2] "An assessment of the near-term viability of accommodating wireless broadband systems in the 1675–1710 MHz, 1755–1780 MHz, 3500–3650 MHz, 4200–4220 MHz and 4380–4400 MHz bands," U.S. Department of Commerce, National Telecommunications and Information Administration, Oct 2010. [Online]. Available: http://www.ntia.doc.gov/files/ntia/publications/fasttrackevaluation_11152010.pdf

[3] "Operation and maintenance instructions, organizational level, radar set AN/SPN-43C," Naval Air Systems Command, Technical Manual, EE216-EB-OMI-010, vol. 1, Sept 2005.

[4] M. G. Cotton and R. A. Dalke, "Spectrum occupancy measurements of the 3550–3650 megahertz maritime radar band near San Diego, California," National Telecommunications and Information Administration, Technical Report TR 14-500, Jan 2014. [Online]. Available: http://www.its.bldrdoc.gov/publications/2747.aspx

[5] F. H. Sanders, J. E. Carroll, G. A. Sanders, and L. S. Cohen, "Measurements of selected naval radar emissions for electromagnetic compatibility analyses," National Telecommunications and Information Administration, Technical Report TR 15-510, Oct 2014. [Online]. Available: http://www.its.bldrdoc.gov/publications/2781.aspx

[6] P. Hale, J. Jargon, P. Jeavons, M. Lofquist, M. Souryal, and A. Wunderlich, "3.5 GHz radar waveform capture at Point Loma," National Institute of Standards and Technology, Technical Note 1954, May 2017. [Online]. Available: https://doi.org/10.6028/NIST.TN.1954

[7] P. Hale, J. Jargon, P. Jeavons, M. Lofquist, M. Souryal, and A. Wunderlich, "3.5 GHz radar waveform capture at Fort Story," National Institute of Standards and Technology, Technical Note 1967, October 2017. [Online]. Available: https://doi.org/10.6028/NIST.TN.1967

[8] *Requirements for Commercial Operation in the U.S. 3550-3700 MHz Citizens Broadband Radio Service Band*, Wireless Innovation Forum, May 2018, Working Document

WINNF-TS-0112, Version V1.5.0. [Online]. Available: https://workspace.winnforum.org/higherlogic/ws/public/download?document_id=6531&filename=WINNF-TS-0112-V1.5.0+CBRS+Operational+and+Functional+Requirements.pdf

[9] F. H. Sanders, J. E. Carroll, G. A. Sanders, R. L. Sole, J. S. Devereux, and E. F. Drocella, "Procedures for laboratory testing of environmental sensing capability sensor devices," National Telecommunications and Information Administration, Techincal Memorandum TM 18-527, November 2017. [Online]. Available: https://www.its.bldrdoc.gov/publications/3184.aspx

[10] W. M. Lees, A. Wunderlich, P. Jeavons, P. D. Hale, and M. R. Souryal, "Deep learning classification of 3.5 GHz band spectrograms with applications to spectrum sensing," *submitted*, Preprint: https://arxiv.org/abs/1806.07745.

[11] S. K. Mitra, *Digital Signal Processing: A Computer-Based Approach*, 3rd ed. New York: McGraw Hill, 2006.

[12] H. L. Van Trees, *Detection, Estimation, and Modulation Theory, Part I*. New York: John Wiley & Sons, 1968.

[13] C. E. Metz, "Basic principles of ROC analysis," *Semin. Nucl. Med.*, vol. 8, pp. 283–298, 1978.

[14] A. Agresti and B. A. Coull, "Approximate is better than "exact" for interval estimation of binomial proportions," *The American Statistician*, vol. 52, no. 2, pp. 119–126, 1998.

[15] L. Wasserman, *All of statistics: A concise course in statistical inference*. New York: Springer, 2004.